UNIVERSITY OF SALERNO

DEPARTMENT OF INDUSTRIAL ENGINEERING

Ph.D. Course in Industrial Engineering
Curriculum in Mechanical Engineering - XXXIII Cycle

Applications of Artificial Neural Network models to Energetic and Propulsion Systems

Supervisor
Prof. Cesare Pianese
Prof. Ivan Arsie

Ph.D. student
Augusto Tortora

Scientific Referees
Prof. Alessandra Perna – University of Cassino and southern Lazio
Prof. Andrea Unich - University of Campania "Luigi Vanvitelli"

Ph.D. Course Coordinator
Prof. Francesco Donsì

Ad una persona,
che mi ha sostenuto ed incoraggiato in una fase della mia
vita molto delicata e che mi ha regalato sempre una
speranza quando sembrava non esserci.

Index

Figure index

Table Index

Abstract

This research work is focused on the application of Artificial Neural Network (ANN) models for the calculation of performance and emissions in two different energy systems:

Diesel engine, in the Automotive sector and Boiler equipped with a Stirling engine, which constitutes a Micro-cogeneration system, in residential building applications.

These two technologies in their respective application contexts, contribute to the pollution of urban areas, due to their harmful emissions for human health. There is therefore a need to reduce emissions, which is in contrast with customer expectations, which require products with ever higher performance and lower consumption.

It is therefore up to designers and manufacturers to find the right trade-off, using technological research and modeling.

Modeling turns out to be a valid tool in the development and management of energy systems, as it allows to minimize the experimental tests and allows to predict the behavior of such systems.

Among the models in the literature, Artificial Neural Networks of the Feed-Forward type have been implemented, which have a continuous functional structure, reduced calculation times and are suitable as objective functions in optimization algorithms.

In the case of the diesel engine, Artificial Neural Network models are developed to infer a prediction of specific fuel consumption, Mean Indicated Pressure (IMEP), NOX and soot emissions. The training of the ANNs was carried out on the basis of experimental datasets, representative of the entire operational plan, deriving from experimental campaigns conducted prior to the present research work.

The obtained models show good continuity and generalizability, with correlation coefficients between 0.97 and 0.99, and are suitable to be implemented in the engine control unit.

In the case of the micro-cogeneration system, the Artificial Neural Network models were conceived as part of an integrated software for the remote management of the entire plant.

The ANN model can effectively simulate the behavior of the boiler system and optimize parameters such as fuel quantity and load rate to achieve the desired performance, in terms of efficiency and CO2 emissions.
The advantages gained from the implementation of the integrated software for the management of the cogenerator lead to energy savings of up to 40% through the use and remote regulation of electronic thermostatic valves; a reduction from 0.3% to 2.0% of the specific consumption of methane in the boiler and a reduction from 10% to 20% of polluting emissions.

Introduction

Context and motivation

The Earth's warming due to the excessive presence of greenhouse gases in the atmosphere, seriously endangers the life on the planet of all living species. The sectors most involved in this phenomenon are those related to industrial production, transport and energy production.

In general, from a combustion reaction complete or incomplete, the presence of products related to it arises. These products are in the form of gas (CO2, CO, NOX, HC), biphasic liquid-gas (water vapour) and solid (solid particulate matter).

Each of these products, if present in high concentrations, can have consequences both on the environment and on human health:
carbonic dioxide (CO_2), damages the ozone layer and is one of the main causes of the greenhouse effect (Töbelmann & Wendler, 2020);

- carbon monoxide (CO), is formed in incomplete combustion due to lack of oxygen, the most present pollutant in the atmosphere, binds to hemoglobin in the presence of oxygen, hindering tissue oxygenation (ARPA FVG , 2019);
- nitrogen oxides (NO_x), are formed in the event of high temperature combustion processes, are responsible for "photochemical smog" and acid rains, have an oxidizing and irritating effect on the eyes, mucous membranes and lungs (Chen, et al., 2007);
- unburned hydrocarbons (HC), which are formed in the event of incomplete combustion, are mainly responsible for "photochemical smog", cause asthma and breathing difficulties (Ogur & Kariuki, 2014).
- water vapor, the most widespread "greenhouse gas", helps to retain infrared radiation, is disposed of in 20 days, the main cause is the water cycle, therefore it is essential for the presence of life on Earth;

- particulate matter, consists of volatile nanoparticles, is formed in the event of rich combustion at high pressures, deposited inside the pulmonary alveoli (Ogur & Kariuki, 2014).

The reaction from the Governments has been to issue increasingly stringent regulations in terms of emissions.

In particular, the European Union has launched a series of increasingly stringent regulatory frameworks to control and limit vehicle emissions.

These regulations in force in Europe are classified by the Euro prefix and by the number relating to the reference standards. To meet these standards, cars must pass tests in which driving cycles are reproduced on test rigs. Until 2017, the reference driving cycle was the NEDC cycle, acronym for New European Driving Cycle, replaced by the WTLP (Worldwide Harmonized Light Vehicles Test Procedures).

This has led to the introduction of technological solutions such as hardware and software technologies to reduce and control the aforementioned emissions.

Among the hardware solutions for the transport sector and, in particular for internal combustion engines, two major examples are the electronic injection device (e.g., Common-Rail) and the exhaust gas after-treatment systems (Arsie, et al., 2004).

As regards the sector relating to energy production, the use of renewable energy and the rational use of non-renewable resources is fundamental. With respect to the latter issue, the solutions adopted relate to cogeneration plants suitable for the simultaneous production of electrical and thermal energy.

In the energy production sector is concerned, there are different needs to be met depending on the energy sources used, the size of the plant and the application.

The energy sources differ in systems powered by renewable energy sources, which are discontinuous over time, and systems powered by non-renewable feedstocks, such as oil and its derivatives, which have the characteristic of guaranteeing continuity in the production of energy.

The size of the considered energy system ranges from the boiler for the production of thermal energy in an apartment to the nuclear power plant for the energy supply of a large region. It is worth recalling that the efficiency of thermal plants is limited by the Carnot's law and could reach values that may range from 0.3 up to 0.55[1].

With the objective of maximizing the overall primary energy conversion factor, cogeneration systems have been developed; cogeneration plants simultaneously generate mechanical and thermal energy. It is worth recalling that for cogeneration systems the energy conversion efficiency could not be used as a reference figure since the theory states that that it is the ratio between mechanical work and thermal energy supplied, whereas in the cogeneration

[1] These efficiency values are given as a broad reference and depends on the size, the power generated and the reference thermodynamic cycle.

the rejected heat is an useful product. For cogeneration plants it is used the ratio of the sum of mechanical work and the recovered thermal energy with respect to the thermal energy supplied.

Within this category, micro-cogeneration systems are created for domestic applications. Their use turns out to be interesting both for consumers, who for the same consumption obtain both a share of mechanical energy and electrical energy, and for the environment, as this has a positive impact on polluting emissions.

In fact, regulatory bodies in Italy and at European level are proposing economic incentives, while enforcing regulatory frameworks concerning the energy efficiency of buildings.

Therefore, the efficiency improvement mainly affects two aspects:

- the improvement of the thermal insulation of the building, consisting of walls and fixtures;
- the adoption of more efficient thermal and electric energy production systems compared to the existing ones.

This latter point has recently led to the adaptation of conventional systems, such as condensing boilers, to micro-cogeneration systems, coupling with Stirling engines, for the conversion of excess thermal energy into electrical energy.

For the management and control of this type of micro-cogenerator, the use of IT systems is essential; it acts as a link between the user, the energy manager and the hardware of the heating system.

At the same time, on one side an increasingly faster internet network (5G) has favored the collection of big data through cloud technologies and has put technologies of different nature (Internet of Things) into communication, while, on the other side, the development of increasingly faster processors in terms of calculation times has made it possible to use artificial intelligence techniques, such as deep-learning and Neural Networks (Patterson, 1999) for the modeling, control and optimization of systems in the energy sector.

Objectives

The objective of this research activity is the application of Artificial Neural Network technologies in the context of two different systems for generating mechanical, electrical and thermal energy. The work is divided into two parts: the first part presents the development of Artificial Neural Networks to model the performance of a Diesel engine for mobility use, whereas the second part deals with the use of Artificial Neural Networks for the management of a small cogeneration system.

The Artificial Neural Networks for Diesel engine models performance variables such as indicated mean effective pressure ($IMEP$) and specific fuel consumption (SFC), pollutant emissions (NO_x and soot), as well as noise emissions for a commercial Common-Rail Diesel Engine (Di Leo, 2015).

Previous research activities and bibliographic analysis suggested to implement black-box models (Spriet & Vansteenkiste, 1988) as objective functions in optimization algorithms of greater use in the industrial field. Among the various models, Feed-Forward Artificial Neural Network models (Hornik, 1991) have been chosen, as they offer excellent performance in terms of precision, generalizability and derivability, compared to other techniques, such as regression (Patterson, 1999).

Based on the experimental data available at the eProLab Laboratory of the University of Salerno, Neural Networks with only one Hidden Layer have been adopted; the activation function of each neuron of this layer is the sigmoid one. The experimental points have been previously prefiltered, in order to remove the outliers and use the points with greater information content. After that, three patterns of input variables were obtained by applying correlation analysis.

For each scheme, several Neural Networks have been calibrated (training phase) to define the optimal number of neurons for the Hidden Layer. The Artificial Neural Network training was divided in two distinct phases: the first phase uses early-stopping techniques (Arsie, et al., 2001) to find the optimal division of entire Dataset in three subsets (training, validation and test); during the second phase the initial values of weight and bias have been varied in order to obtain the network with the best correlation coefficient (Mastroberti & Pianese, 2000).

In the second part of the thesis, Artificial Neural Networks have been used to manage and optimize the following aspects of interest for conventional boilers (Cutler, et al., 2014) equipped with Stirling engine (Zhu, et al., 2021), for the generation of electricity (Combined Heat and Power – CHP). Therefore, main points tackled deal with:

- anomalies and maintenance interventions;
- energy consumption;
- fluids;
- fumes.

In particular, the objective is to create a system for water heating in which the energy production phase is based on boilers operating in cogeneration mode (i.e., producing electrical and thermal energy at the same time). From the data taken from the boiler, Artificial Neural Networks have been implemented and a preliminary methodology based on linear regression has been proposed for the reduction of the parameter space. This allowed obtaining predictive models to be used in future computer systems for the remote management of such a cogenerator in residential buildings and houses.

Contribution and innovation of this research work

Artificial Neural Network models are becoming very popular for their effective use in many industrial sectors, as there is the possibility of

overcoming the technological limits, which prevented in the past their use in practical applications and products. In fact, the diffusion of Cloud technologies has made it possible to collect large quantities of data in Data Centers located around the globe. This is also thanks to the development of network infrastructures with communication speeds of up to 1.8 Gbit/s (5G), which allow for fast and effective transmission.

Alongside this, the creation of multicore processors has made it possible to implement parallel computing, which exponentially reduces training times.

The determining factor for the on board implementation for automotive applications lies in the development of processors for control units containing circuits dedicated to the resolution of optimization and control problems in times of the order of milliseconds.

The present work focuses on this specific application field, which today is intended for the prediction of the behavior of a Diesel engine, but which in the future can be re-adapted, through a recalibration of the parameters, for different types of engines.

The parameter calibration procedure was divided into two phases:

- research based on the combination of data in training, validation and test sets.
- the variation of the initial value in the training phase of the parameters of the Neural Network (weights and bias).

In the case of the micro-cogenerator, the network is part of an integrated computer system and is placed within a process that combines closed-loop control and optimization of efficiency and emissions. Moreover, in this case the contribution of the work and the methodologies implemented aim to be used for different classes of micro-cogenerators for domestic use.

CHAPTER 1
Internal Combustion Engines

Internal combustion engines convert chemical energy into mechanical energy through a combustion reaction. Unlike the other propulsion systems, the internal combustion engines have a high elasticity of operation and for this reason they are used in the automotive and transport sector (Arsie, et al., 2004). In this context, variable power and variable torque are required due to the discontinuity of the road surface and its slope, variable vehicle traffic, different driving style, etc. A classification can be made according to the type of reference thermodynamic cycle, in particular with respect to the combustion phase (heat adduction), which can occur at constant volume or constant pressure. In the first case there are compression-ignition or Diesel-cycle engines (Di Leo, 2015), in the second case those with spark ignition or Otto cycle engines (Arsie, et al., 1999).

Diesel engines have a higher thermodynamic efficiency, since it is possible to achieve higher pressures and temperatures in the chamber than a spark ignition engine, where compression ratios must be reduced to avoid the occurrence of some instability phenomena such as detonation.

With the introduction of mechanical supercharging systems (turbo-compressor), of electronic injection management and of common-rail systems, it has been possible to achieve comparable and, sometimes, higher powers than those provided by the spark injection engines with lower fuel consumption and CO_2 emissions. In fact, according to the European Automobile Manufacturers Association, Diesel engines burn 30% less fuel on average and emit 25% less CO_2 than gasoline engines.

Nevertheless, in a compression-ignition engine, emissions of some sub-products of the combustion reaction are higher.

The regulation of European Union pushes the automotive industries to pay more attention to polluting emissions, which have been reduced through the introduction of catalysts, particulate filters and Exhaust Gas Recirculation

circuits (EGR) within the combustion chamber. Such hardware solutions, if assisted with optimally tuned engine control parameters can bring benefits by reducing emissions and consumption, while improving other engine performance metrics (eg., torque).

The control parameters are supplied by the manufacturer to the engine control unit during the design phase, among other the main variables are:

- the amount of fuel to be injected;
- the number of injections;
- the injection angle;
- the injection pressure;
- the opening of the EGR valve;
- the position of the turbine stator blades (VGT).

The calibration of these parameters is carried out either experimentally or with models. Mathematical models replace experimental tests, because they can represent a physical phenomenon in times and lowering the costs of experimental activities (Arsie, et al., 2001).

In the next section the main parameters for evaluating the performance of an engine and the reference regulatory framework are described.

1.1 Control and performance parameters of Diesel engines

As anticipated above, modern Diesel engines are equipped with some hardware solutions (Figure 1-1), that have increased performance and have reduced consumption and emissions.

In order to increase performance in terms of thermodynamic work the turbocharger is introduced. With the same scope and for the purpose to reduce fuel consumption, by means of an optimal management of combustion process, systems like Common-Rail and electro-injectors have been adopted.

The reduction of emissions is obtained with some devices:

- the EGR circuit and SCR (Selective Catalyst Reduction) for the reduction of nitrogen oxides (NOx);
- the Diesel Particulate Filter (DPF) for the reduction of particulate matter ($soot$);
- the Diesel Oxidation Catalyst (DOC catalyst) for the oxidation of carbon monoxide (CO) and the unburned hydrocarbons (HC).

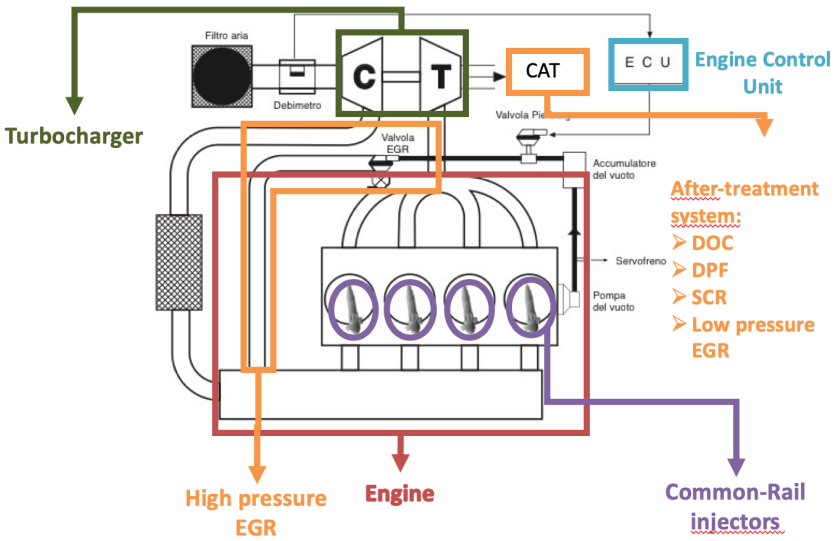

Figure 1-1 Scheme of the Diesel Engine with the main systems and devices that have enhanced the performance and reduced the emissions.

All these devices are controlled by the Engine Control Unit (ECU) which is a computer that sets the control parameters by using maps and on-board algorithms. The ECU takes electric signals in input and feeds electric signals to the actuators. The signals in input come from the measurement devices installed on the engine, such as flow meter, temperature and pressure sensors. The output signals go to the actuators like injectors, EGR valve, VGT (Variable Geometry Turbine).

For the management of input and output variables, tuning activities are needed to find the optimal values of the following control (C) and measured (M) parameters:

- **Speed** (M)**,** measured in rpm, is the speed of crankshaft's rotation, its steady state value depends on the equilibrium between engine delivered torque and the sum of all resistance torques; torque and *rpm* identify the operating conditions;
- **Number of injections (C)**: from 1 to 5 injections, that are named Pilot, Pre, Main, After, Post (*name of injection*) in a temporal injection ordering (see Figure 1-2); for the sake of clarity, henceforth those names are used as subscripts of the variables concerned;
- **Quantity of fuel** ($Q_{name\ of\ injection}$) (C) as volume flow injected in the cylinder for each injection expressed in $\frac{mm^3}{stroke}$;

- **Start of each injection** ($SOI_{name\ of\ injection}$) (C) measured in $degBTDC$ (degree Before Top Dead Center), that indicate the time when injection takes place;
- **Dwell time** ($DT_{name\ of\ injection}$) (C) measured in μs, that indicates the time interval from the considered injection and the start of the following one;
- **Rail pressure** (P_{rail}) (C) measured in bar, that indicates the pressure of the fuel injected in the cylinder;
- **EGR valve opening percentage (C)**, that indicates indirectly the quantity of exhaust gas recirculating from the exhaust pipeline to manifold, that is the volume near the inlet valve of engine; the exhaust gas recirculated is useful to reduce the maximum temperature during the combustion phase and, as a consequence, reduces NO_X emissions, as well as both the available thermodynamic work and the efficiency;
- **VGT opening percentage (C),** that indicates indirectly the quantity and the speed of exhaust gas;
- **Air mass in** Kg/s (M) indicates the air flow rate at the inlet valve.

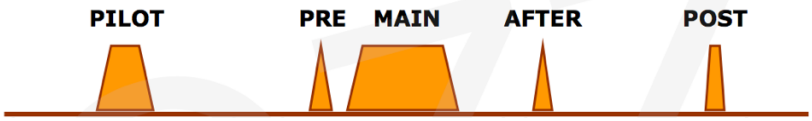

Figure 1-2 Injection in a Diesel engine

In order to obtain the optimal conditions in terms of performance and consumption, the variables to be estimated are the Indicated Mean Effective pressure ($IMEP$) and the Specific Fuel Consumption (SFC).

The Indicated Mean Effective Pressure (IMEP) gives information about the work per displacement (V_D) unit and is calculated as the mean integral value of pressure ($p(v)$) with respect to the volume (v):

$$IMEP = \frac{1}{V_D} \oint_{cycle} p(v)\, dv \qquad (1.1)$$

The Specific Fuel Consumption indicates the quantity of fuel per unit of useful energy from engine or the flow fuel mass per power unit:

$$SFC = \frac{m_{inj\ TOT}}{\eta_m * IMEP * V_D} \qquad (1.2)$$

where $m_{inj\,TOT}$ is the mass of fuel injected during a thermodynamic cycle and η_m is the mechanical efficiency (Tortora, 2017).

1.2 Reference regulatory framework

Polluting and acoustic emissions are included in a regulatory framework that has tightened in the last decades, limiting the placing on the market of new vehicles. The purpose of these legislations is to make urban environments more livable, limiting the release of toxic emissions thus preventing the occurrence of severe and even lethal diseases in humans. These regulations are in force in Europe and are classified by the prefix Euro and the number relative to the reference standards (see Table 1-1 and Figure 1-3). To meet these standards, cars must pass tests in which driving cycles are reproduced on test benches. Until 2017, the reference driving cycle was the NEDC cycle, which stands for the New European Driving Cycle and was replaced by the WTLP (Worldwide Harmonized Light Vehicles Test Procedures).

Table 1-1 Evolution of emission limits in European regulatory framework. (Tortora, 2017)

Emission level and year of enforcement		Test procedure	CO (g/KWh)	HC (g/KWh)	NMHC (g/KWh)	CH4 (g/KWh)	NOX (g/KWh)	PM (g/KWh)
Euro VI	2014	Steady state	1,5	0,13			0,4	0,1
		Transient	4		0,16	0,5	0,46	0,1
Euro V	2008	Steady state	1,5	0,46			2	0,02
		Transient	4		0,55	1,1	2	0,03
Euro IV	2005	Steady state	1,5	0,46			3,5	0,02
		Transient	4		0,55	1,1	3,5	0,03
Euro III	2000	Steady state	2,1	0,66			5	0,1
		Transient	5,45		0,76	1,6	5	0,16
Euro II	1996	Steady state	4	1,1			7	0,15
Euro I	1991	Steady state	4,5	1,1			8	0,36
Euro 0		Steady state	11,2	2,4			14,4	

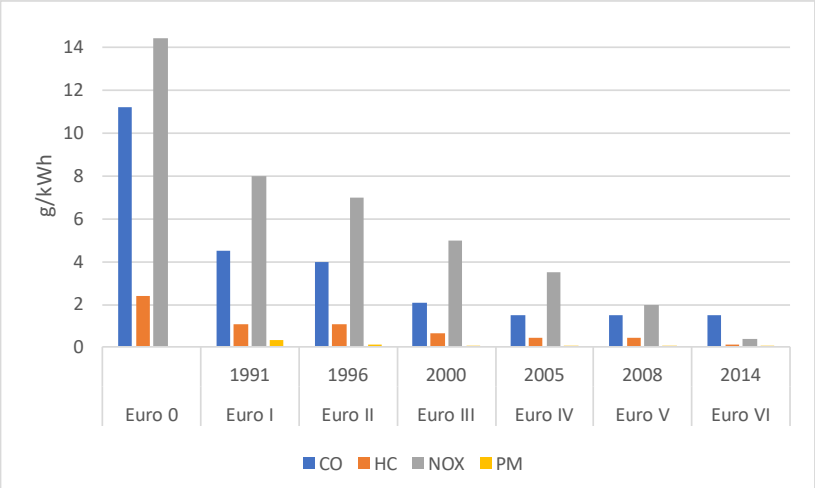

Figure 1-3 Emission trend in European regulatory Framework. (Tortora, 2017)

From the figures, it is possible to notice that NOx emissions are reduced by two orders of magnitude from the Euro 0 to the Euro 6, losing an order of magnitude only from Euro 5 to Euro 6. As regards the emissions of particulate matter the framework is focused on reducing the dimensions of particles, because they are the most dangerous for the pulmonary alveoli; the tolerated value has gone from $0.36\frac{g}{KWh}$ of Euro 1 to $0{,}01\frac{g}{KWh}$ of Euro 6, and this value is divided by two in the changeover from Euro 5 and Euro 6. Instead, after a sharp decrease between Euro 0 ($11.2\frac{g}{KWh}$) and Euro 4 ($1.4\frac{g}{KWh}$), CO emissions have remained constant in the subsequent regulatory frameworks, while the unburned hydrocarbons have lost only one order of magnitude between Euro 2 and Euro 6 (Tortora, 2017).

CHAPTER 2
Combined Heat and Power

Another application of the Diesel engine is in stationary applications like a generator in Combined Heat and Power (CHP) plant for the production of electric and thermal energy for hot sanitary water and hot air in a building. (Zhu, et al., 2021)

CHP, or “cogeneration”, implies that heat and electricity are produced simultaneously in one process. The use of combined heat and power helps to improve the overall efficiency of electricity and heat production as these plants combine electricity production technologies with heat recovery equipment. Increasing the conversion efficiency of power generation through the use of CHP helps to reduce the environmental impact of power generation. A higher penetration of CHP will also help achieving the 20% target for Green House Gas (GHG) emissions, the 20% target for renewable energy in final energy consumption and the 20% reduction in gross inland consumption compared to a Business-as-usual (BAU) scenario by 2020 (Bianchi, et al., 2014). CHP has received policy support in the latest proposed package on the Energy Efficiency Directive, which is now being scrutinized by the Council and by the European Parliament.

If adopted, this package will more closely integrate CHP with efficiency in transformation and distribution (ENER 11) and the overall efficiency of thermal generation (ENER 19) (Sokołowski, 2020) (European Enviroment Agency, 2010).

CHAPTER 2

2.1 Types of plants

Several configurations have been developed in the years to build CHP plants to maximizes the production of both electricity and heat according to the use of each application. Produced work and thermal energy recovered depend upon the thermal cycle of the plant and thus the amount of primary energy (i.e., fuel) converted.

Topping cycle plants primarily produce electricity from a steam turbine. Partly expanded steam is then condensed in a heating condenser at a temperature level that is suitable for the uses of the recovered heat, e.g. (Wang, et al., 2019) or water desalination.

Bottoming cycle plants produce high temperature heat for industrial processes; then, a waste heat recovery boiler feeds an electrical plant. Bottoming cycle plants are only used in industrial processes that require very high temperatures such as furnaces for glass and metal manufacturing, so they are less common.

Large cogeneration systems provide heating water and power for an industrial site or an entire town. Common plant types are CHP (Zhu, et al., 2021), (Martinez, et al., 2017):

- gas turbine CHP plants using the waste heat in the flue gas of gas turbines; the fuel used is typically natural gas;
- gas engine CHP plants use a reciprocating engine, which is generally more competitive than a gas turbine up to about 5 MW. The gaseous fuel used is normally natural gas. These plants are generally manufactured as fully packaged units that can be installed within a plantroom or external plant compound with simple connections to the site's gas supply, electrical distribution network and heating systems;
- biofuel engine CHP plants use an adapted reciprocating gas engine or Diesel Engine, depending upon which biofuel is being used, and are very similar in design to a Gas engine CHP plant. The advantage of using a biofuel engine is the reduced hydrocarbon fuel consumption and thus the reduced carbon emissions. These plants are generally manufactured as fully packaged units that can be installed within a plantroom or external plant compound with simple connections to the site's electrical distribution and heating systems. Another variant is the wood gasifier CHP plant whereby a wood pellet or wood chip biofuel is gasified in a zero oxygen high temperature environment; the resulting gas is then used to power the gas engine;
- combined cycle power plants adapted for CHP;

- molten-carbonate fuel cells and solid oxide fuel cells have a hot exhaust, very suitable for heating;
- steam turbine CHP plants that use the heating system as the steam condenser for the steam turbine;
- nuclear power plants, similar to other steam turbine power plants, can be fitted with extractions in the turbines to bleed partially expanded steam to a heating system. With a heating system temperature of 95 °C it is possible to extract about 10 MW heat for every MW electricity lost. With a temperature of 130 °C the gain is slightly smaller, about 7 MW for every electric MegaWatt (MWe) lost.

Smaller cogeneration units may use a reciprocating engine or Stirling engine. The heat is removed from the exhaust gases and from the cooling fluid. These systems are well suited for low power applications because small gas and Diesel engines are less expensive than small gas- or oil-fired steam-plants.

Some cogeneration plants are fired by biomass, or industrial and municipal solid waste (e.g., incineration). Some CHP plants utilize waste gas as the fuel for electricity and heat generation. Waste gases can be gas from animal waste, landfill gas, gas from coal mines, sewage gas, and combustible industrial waste gas.

Some cogeneration plants combine gas and solar photovoltaic generation to further improve technical and environmental performance. Such hybrid systems can be scaled down to the building level and even to individual homes (Wikipedia, 2021).

2.2 The micro-CHP technology

Micro-CHP is a vast class of low power CHP systems. As for large size CHP, the same principle is exploited to increases energy efficiency, by converting primary energy to heat and electricity at the end-user level. Energy losses are minimized since heat losses at central electricity production facilities and network losses in the electricity grid are avoided.

Micro-CHP products produce heat and electricity simultaneously based on a range of technologies. They can be categorized in three groups (see also Figure 2-1):

- internal combustion;
- External combustion;
- chemical conversion (fuel cells).

Each technology has its unique properties and thereby serving different kinds of end-users and markets (CODE 2, 2014).

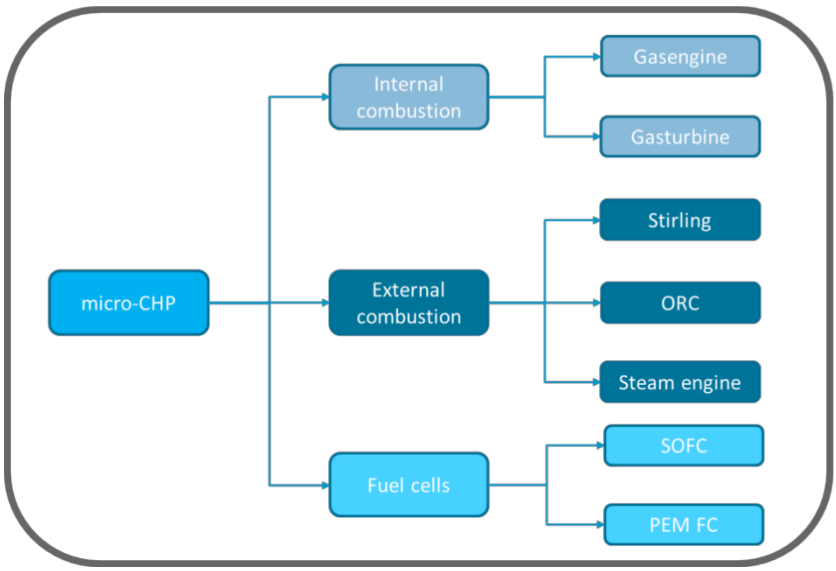

Figure 2-1 Micro-CHP technologies (CODE 2, 2014).

Table 2-1 Comparison of different heating technologies for the built environment (CODE 2, 2014).

	Application			Existing connection		Fit with existing heat exchangers	Other remarks
	Low temperature space heating	High temperature space heating	Hot tap water	Fit with gas connection	Fit with electric connection		
Condensing boiler	V	V	V	V		V	No major efficiency improvements to be expected
Ground source heatpump	V	X	X		V	X	Yearly balance of ground source
Air source heatpump	V	X	X		V	X	Feasible in new building or renovation projects
Solar Heat	X	X	V	V		X	Seasonal availability
micro-CHP	V	V	V	V	V	V	
Biomass boiler	V	V	V			V	Biomass (source) availability
District heating	V	V	V			V	Heat network needed

Since a micro-CHP produces relatively high temperature heat, it can be easily implemented in the heating systems of existing buildings. Furthermore, it fits well into the existing gas and electric infrastructure. In Table 2-1, a comparison is made among different heating technologies for the built

environment showing that micro-CHP has the same application areas as a (condensing) boiler and has a unique fit to the market for existing buildings.

In this work, Artificial Neural Network techniques have been implemented to calculate the efficiency and the emissions from micro-CHP boiler, to help managing a domestic system made of a boiler and a Stirling engine (Martinez, et al., 2017).

2.3 Stirling engine Beta-type

The Stirling engine is an external combustion engine, which, in the case analyzed, uses the heat taken from the boiler to produce electricity.

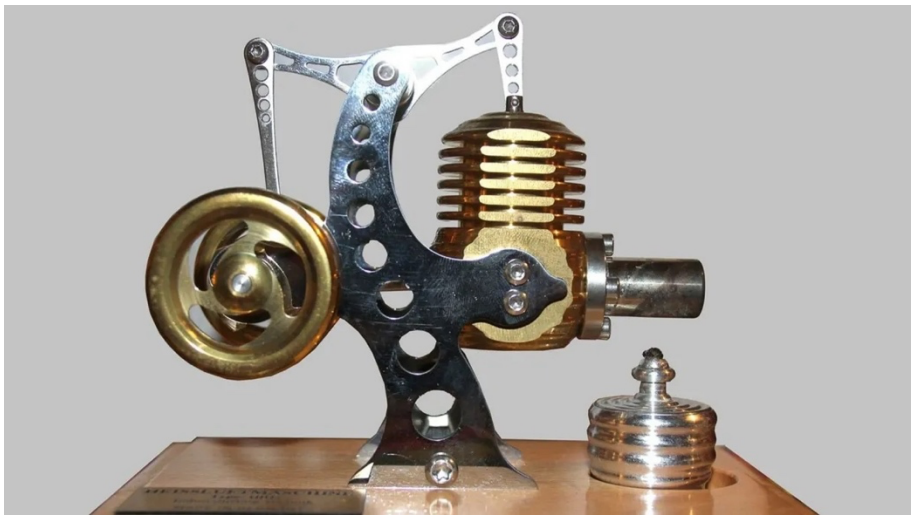

Figure 2-2 Example of Stirling Engine (Interesting Engineering, 2011)

The specific application involves the use of a Beta type Stirling engine in free piston configurations, which guarantees minimum dimensions and high values of efficiency.

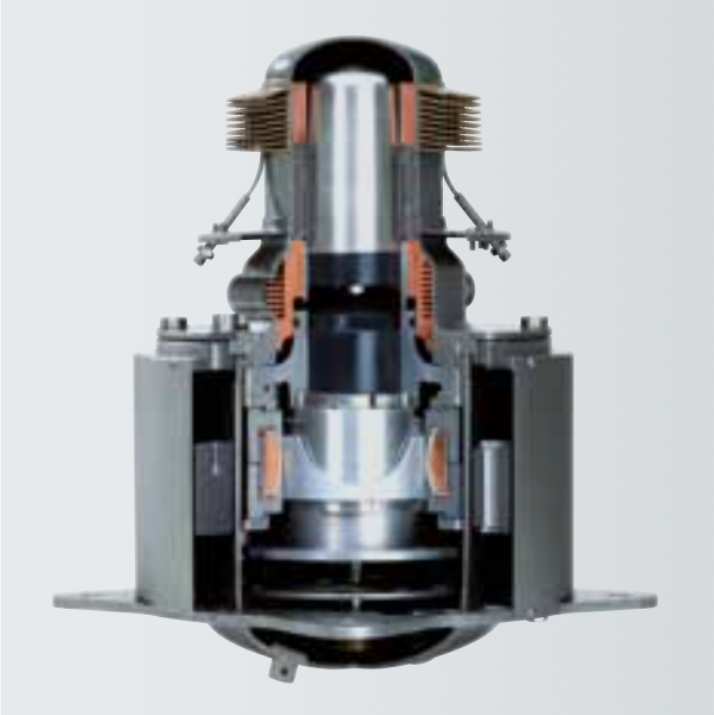

Figure 2-3 Stirling engine Beta-Type in Free Cylinder configuration used in micro-CHP system (The Plan.it, 2012)

In Beta-type configuration, the driving piston and the displacer are contained in the same cylinder and connected to the same crankshaft. The displacer has no side seals, as it is responsible for moving the fluid between the cold and hot chamber. The piston, equipped with seals, cyclically compresses and expands the work fluid. The displacer is offset from the piston by a lag angle of about 90° (see **Figure 2-4**).

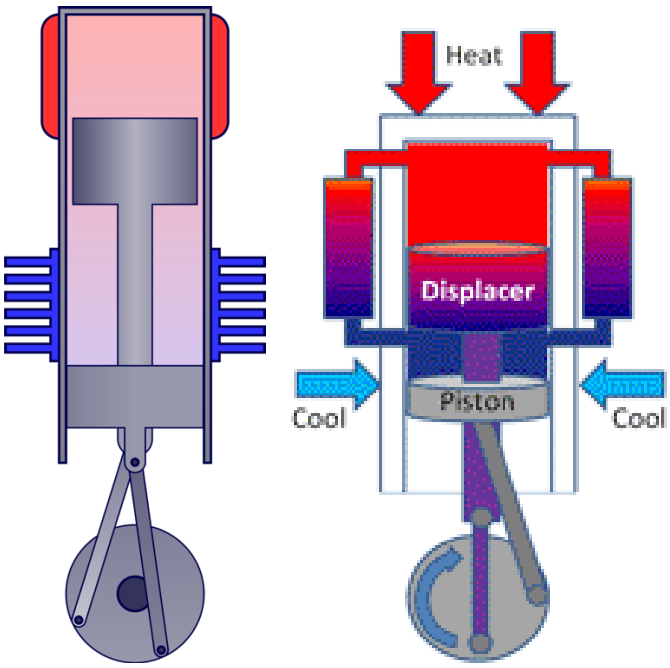

Figure 2-4 Example of Stirling Engine Beta-type (TiKz.net, 2023).

The thermodynamic transformations occurring in a beta-type Stirling (see Figures 2-5 and 2-6) are:

- isothermal compression (1-2): The displacer is fixed at top dead center while the piston is at bottom dead center. All the mass of fluid is contained in the compression volume where the minimum properties of pressure and temperature are obtained. The piston begins its ascent by compressing the fluid;
- isochoric heating (2-3): The displacer begins its descent favoring the passage of the fluid in the lateral channel which represents the regenerator where it absorbs heat. The piston remains stationary ensuring that the available volume remains constant. The heating of the fluid takes place mainly thanks to the heat of the regenerator but reaches the maximum temperature thanks to the hot exchanger in the upper part;
- isothermal expansion (3-4): The fluid is totally transferred into the expansion chamber where it reaches the maximum temperature and pressure conditions. The engine piston reaches top dead center while the displacer reaches bottom dead center;

- isochoric cooling (4-1): The piston begins to descend towards the bottom dead center and after a time defined a priori the displacer also begins to move with the same speed since it is an isochor transformation. The gas returns to the regenerator giving it the same amount of heat it absorbed in the heating phase, then it cools down again thanks to the cold exchanger (Thombare & Verma, 2008).

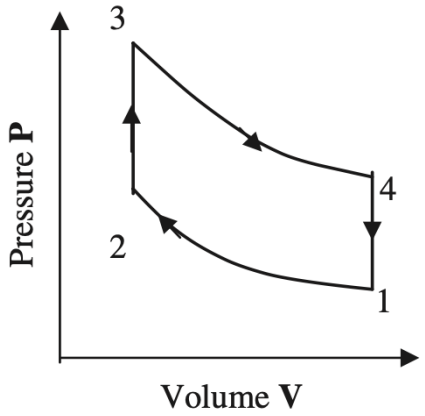

Figure 2-5 Thermodynamic Cycle of Stirling Engine in p-V plane (Thombare & Verma, 2008)

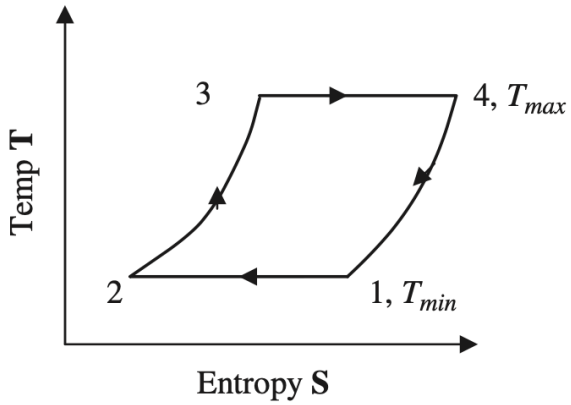

Figure 2-6 Thermodynamic cycle of the Stirling engine in the T-s plane (Thombare & Verma, 2008)

The main advantages of this configuration are:

- Extreme compactness;

- Greater constructive simplicity, because there is only one cylinder[2];
- Possibility of having concentrated seals only for the piston;
- Very low dead volumes;
- High efficiency;
- High specific power.

The disadvantages are:

- Complex optimization of the chambers and the phase angle between the two pistons, due to the contained dead volumes;
- Delayed thermal exchanges;
- The ideal condition on the pistons, i.e that in some cases they remain stationary, cannot be considered real. In fact, in real operation they do not remain stationary, but remain in motion, minimizing dead volumes.

In free-piston configuration, pistons are moved by the pressure forces acting within the engine, so there is no connection between the pistons and the crankshaft.

Typically they are applied to Beta-type Stirling engines and, despite the complexity of the design, have the following advantages:

- reduction of weight and size due to the elimination of the kinematic mechanism;
- absence of external forces, except for the mass forces acting on the pistons in the case where the engine is arranged horizontally;
- no required pistons seals;
- limited friction;
- no external maintenance and high reliability;
- self-start by heating the end corresponding to the expansion chamber

2.4 Boiler with Stirling engine

The micro-CHP system, that is considered in this thesis, is a condensing boiler coupled with a Stirling engine. The condensing boiler provides thermal energy for heating and the production of domestic hot water, while the Stirling engine uses the heat produced by the combustion of methane to produce electricity.

[2] Other configurations, are alpha with two cilinders (one for hot fluid and one for cold fluid) and gamma, that present one cylinder for the piston and one for displacer, to perform the same thermodynamic cycle.

The boiler under examination contains two circuits and therefore two burners to satisfy the peaks in thermal energy demand. The primary circuit feeds the cogenerator and takes care of the production of thermal energy for the production of domestic hot water and medium-low heating loads. The secondary circuit is independent from the first and works simultaneously in order to satisfy the peak loads required during the coldest months of the year.

The functional characteristics of the analyzed boiler and its plant are shown in the Table 2-2, the scheme is shown in Figure 2-7 and table 2-3.

Table 2-2 Functional characteristics of the Boiler with Stirling Engine as sketched in Figure 2-7.

Physical dimension	**Unit**	
Useful potential range in heating		
TM/TR =50°C/30°C	kWth	3,6 – 26
TM/TR = 80°C/60°C	kWth	3,2 – 24,6
Electric Power	kWel	0,99
Efficiency[3]		0,97(Hs)/1,08(Hi)
Length	mm	480
Width	mm	480
Height	mm	900
Weight	kg	120
Heat exchanger water content	l	4
Nominal Voltage	V	220
Nominal Frequency	Hz	50

[3] The efficiency value greater than 1 uses the lower calorific value (H_i) in the denominator, to make it comparable with the efficiency value of traditional boilers. In this case, the latent heat of condensation of the water vapor contained in the fumes is considered as useful energy.

The value that makes physical sense is that of the efficiency obtained considering the higher calorific value, since the latent heat of condensation must be considered in the total calculation of the heat made available by the fuel, which in the considered case is methane. (Energia zero, 2017)

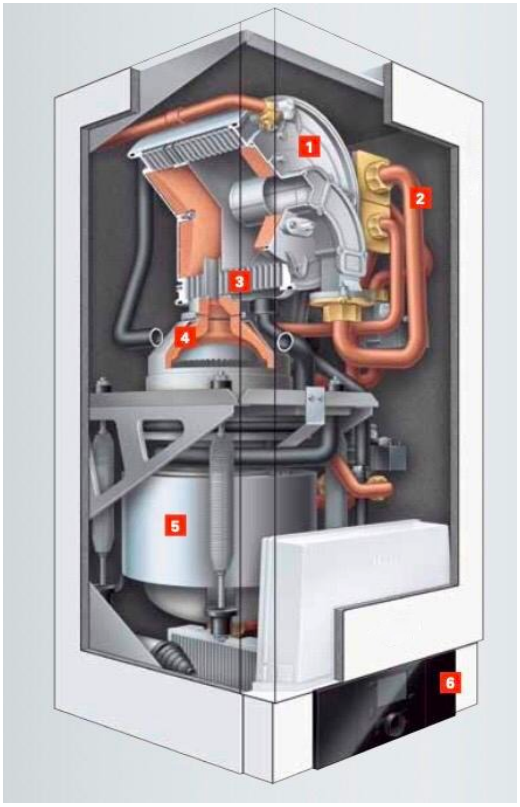

Figure 2-7 Plant of the Boiler with Stirling Engine adapted from (The Plan.it, 2012)

Table 2-3 Description of the plant of the boiler with Stirling Engine (The Plan.it, 2012)

1	Boiler for peak loads
2	Air distribution
3	Radial Heat Exchanger in stainless steel
4	Ring burner
5	Stirling Engine Beta-type
6	Control Panel

CHAPTER 3
Artificial Neural Networks

In this section are recalled the main concepts of Neural Networks. Not all Neural Networks are designed to tackle every problem domain. The parameters described in the previous sections are used in black-box models. This kind of models correlate directly the inputs and outputs using a mathematical function. The advantages of this kind of models are the possibility to have a derivable function and the reduction of the computational time with respect to gray and white box models. The main disadvantage is the large number of experimental data required during implementation and validation phases. (Spriet & Vansteenkiste, 1988)

Among all the black-box models described in the literature, Neural Networks are preferred because they return reliable results in terms of precision and generalizability.

Artificial Neural Networks are algorithms inspired by biological Neural Networks. (Hopfield & Tank, 1985)

The main structure of a Neural Network is characterized by the following three parts (see Figure 3-1):

- Input Layer;
- Hidden Layer;
- Output Layer.

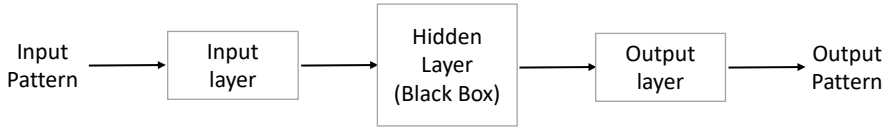

Figure 3-1. General scheme of a Neural Network adapated from (Beale, et al., 2017)

The three layers are linked by some node which takes the name of neuron as shown in Figure 3-2.

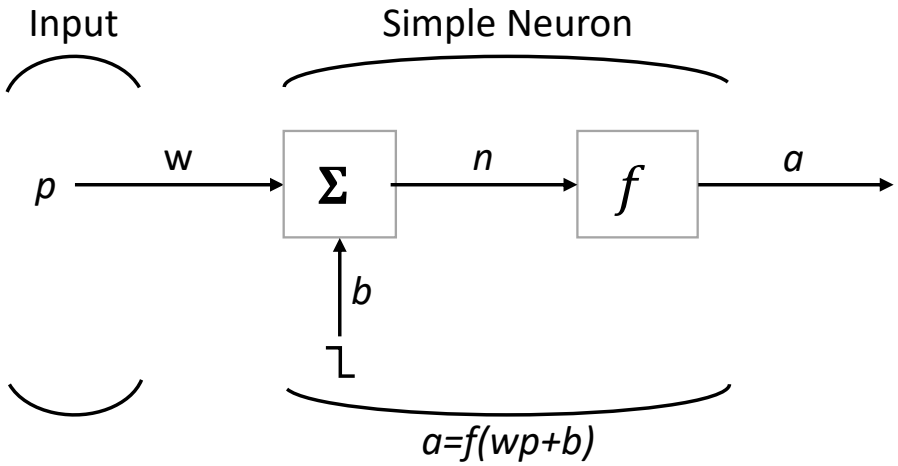

Figure 3-2. Scheme of a single Neuron adapted from (Beale, et al., 2017)

In each neuron three distinct functional operations take place. First, the scalar input p is multiplied by the scalar weight w to form the product wp, again a scalar. Second, the weighted input wp is added to the scalar bias b to form the net input n.

Finally, the net input is passed through the transfer or activation function f, which produces the scalar output a. The names given to these three processes are: the weight function, the net input function and the transfer function. The activation function characterizes the neuron and also the network. Therefore, the neurons are computational elements implemented in each of the three layers and are of three kinds:

- Input Neuron;
- Hidden Neuron;
- Output Neuron.

Input Neurons take data from an array and transfer it to Hidden Neurons, which help the network to understand the input data to the Input Layer and transfer the data at the following Hidden Neurons or at the Output Layer, that transfer the data to the array of output (Patterson, 1999), see Figure 3-3.

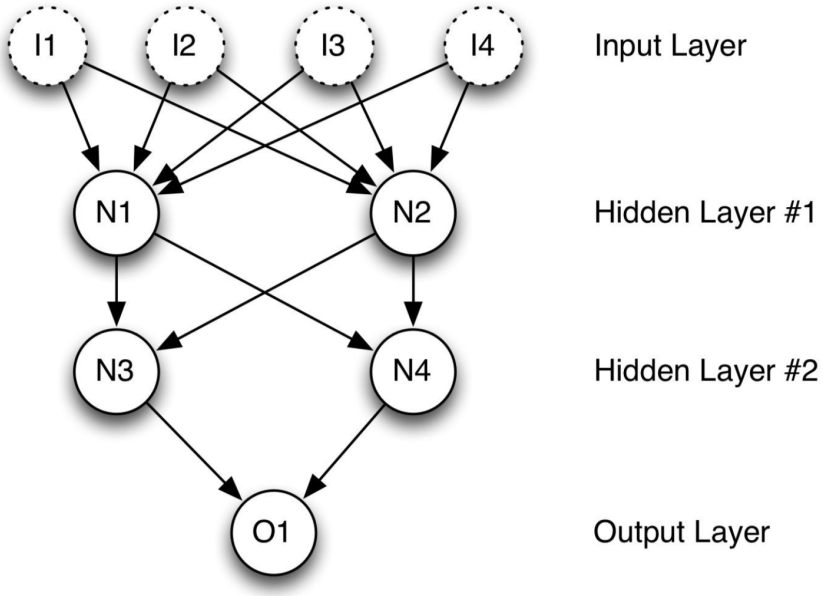

Figure 3-3 Example of Neural Network (Heaton, 2015).

Several types of Neural Network are available in the technical literature. Each Neural Network has its own structure, which is a combination of neurons and layers with internal and external connections whose combinations are purposely defined to solve different problems. Table 3-1 shows the main Neural Network types and their applicable problem domains as specified in the following list (Heaton, 2015):

- Clust – Unsupervised clustering problems;
- Regis – Regression problems, the network must output a number based on input;
- Classif – Classification problems, the network must classify data points into predefined classes;
- Predict – The network must predict events in time, such as signals for finance applications;
- Robot – Robotics, using sensors and motor control;
- Vision – Computer Vision (CV) problems require the computer to understand images;
- Optim – Optimization problems require that the network find the best ordering or set of values to achieve an objective.

Table 3-1 The main types of Neural Networks (Heaton, 2015).

	Clust	Regis	Classif	Predict	Robot	Vision	Optim
Self-Organizing Map	✓✓✓				✓	✓	
Feedforward		✓✓✓	✓✓✓	✓✓	✓✓	✓✓	
Hopfield			✓			✓	✓
Boltzmann Machine			✓				✓✓
Deep Belief Network			✓✓✓		✓✓	✓✓	
Deep Feedforward		✓✓✓	✓✓✓	✓✓	✓✓✓	✓✓	
NEAT		✓✓	✓✓		✓✓		
CPPN					✓✓✓	✓✓	
HyperNEAT		✓✓	✓✓		✓✓✓	✓✓	
Convolutional Network		✓	✓✓✓		✓✓✓	✓✓✓	
Elman Network		✓✓	✓✓	✓✓✓			
Jordan Network		✓✓	✓✓	✓✓	✓✓		
Recurrent Network		✓✓	✓✓	✓✓✓	✓✓	✓	

The number of checkmarks shows the applicability of each of the Neural Network types to that particular problem. If there are no checks, that network type cannot be applied to that problem domain. (Heaton, 2015)

In this work, Feed-Forward Neural Networks have been adopted to calculate:

i. the correlations between control parameters and performance, consumption and emissions in internal combustion engines;
ii. the correlation between efficiency and CO emissions and load for boilers in CHP systems.

3.1 Activation functions

In Neural Network programming, activation or transfer functions establish bounds for the output of neurons. Neural Networks can use many different activation functions, that are described in this paragraph.

3.1.1 Linear Activation Function

The most basic activation function is the linear function, because it does not change the neuron output at all:

$$y = x \tag{3.1}$$

This activation function simply returns the value that the neuron has received as input, as shown in Figure 3-4 (Haykin, 1999).

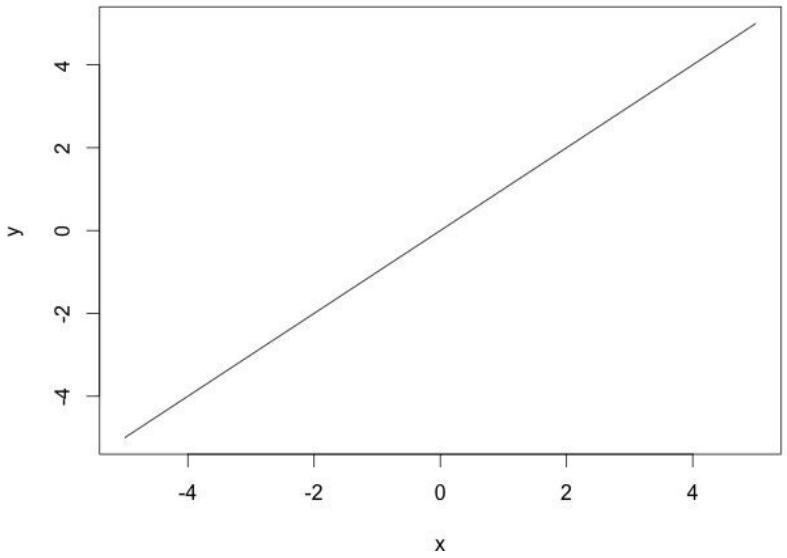

Figure 3-4 The linear activation function (Heaton, 2015).

3.1.2 Step Activation Function

The step or threshold activation function is another simple activation function. Neural Networks were originally called perceptrons McCulloch & Pitts (1943) introduced the original perceptron and used a step activation function like the following:

$$y = \begin{cases} 1, if\ x \geq 0.5 \\ 0\ otherwise \end{cases} \quad (3.2)$$

In this sample definition, the function returns as output a value of 1.0 for incoming values of 0.5 or higher, and 0 for all other values. Step functions are often called threshold functions because they return 1 (true) only for values that are above the specified threshold (McCulloch & Pitts, 1943), as seen in Figure 3-5:

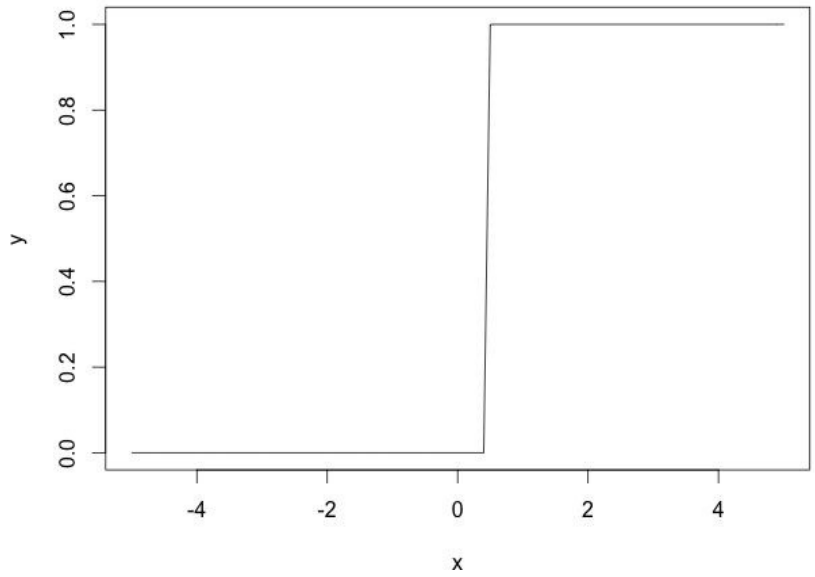

Figure 3-5 Step Activation Function (Heaton, 2015).

3.1.3 Sigmoid Activation Function

The sigmoid or logistic activation function is a very common choice for Feed-Forward Neural Networks that need to output only positive values. Despite its widespread use, the hyperbolic tangent or the rectified linear unit (ReLU) activation function is usually a more suitable choice. The ReLU activation function is described later in this paragraph (Kalman & Kwasny, 1992). The following equation shows the sigmoid activation function:

$$y = \frac{1}{1 + e^{-x}} \qquad (3.3)$$

The use of the sigmoid function ensures that values stay within a relatively small range, as it can be observed in the figure 3-6:

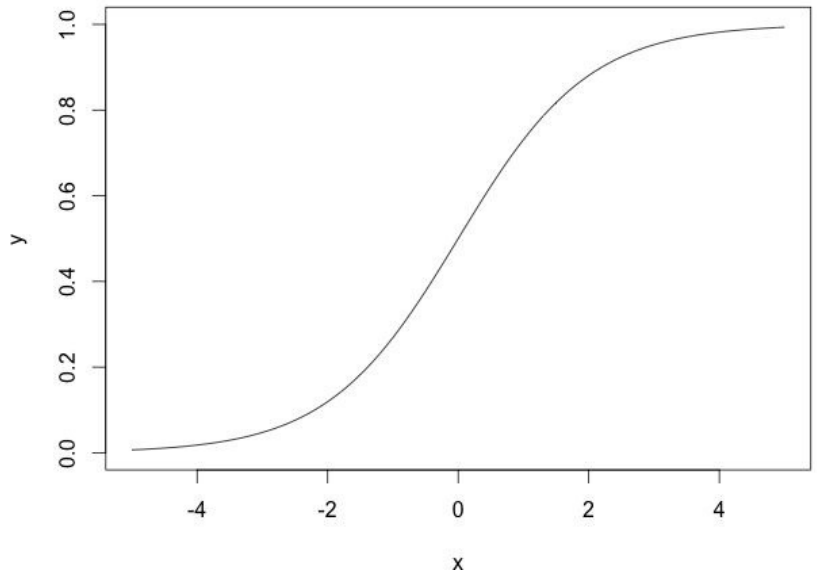

Figure 3-6 Sigmoid Activation Function (Heaton, 2015).

As it is possible to see from the above graph, values above or below 0 are compressed to the approximate range between 0 and 1.

3.1.4 Hyperbolic Tangent Activation Function

The hyperbolic tangent function is also a very common activation function for Neural Networks that must output values in the range between -1 and 1. This activation function is simply the hyperbolic tangent (tanh) function, as shown in the equation (Patterson, 1999):

$$y = \tanh(x) \qquad (3.4)$$

The graph of the hyperbolic tangent function has a shape similar to the sigmoid activation function, as seen in Figure 3-7:

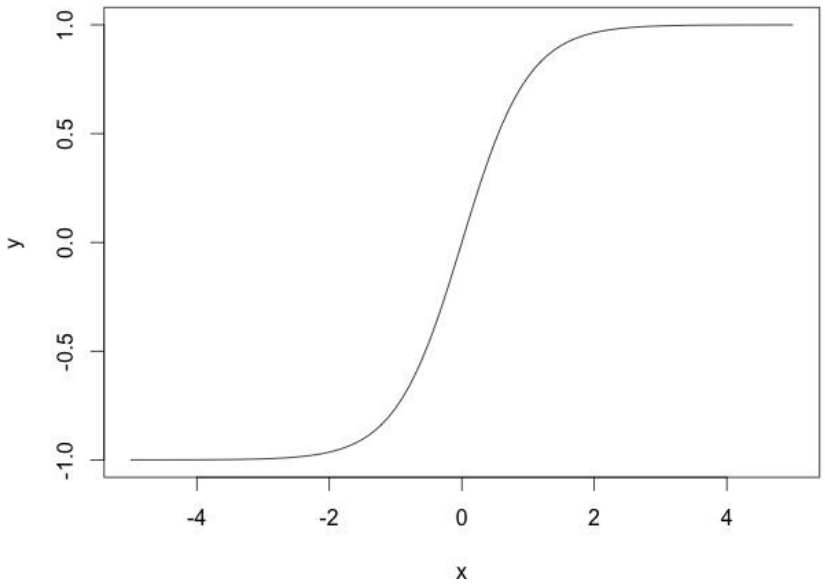

Figure 3-7 Hyperbolic Tangent Activation Function (Heaton, 2015).

The hyperbolic tangent function has several advantages over the sigmoid activation function. These involve the derivatives used in the training of the Neural Network.

3.1.5 Rectified Linear Units (ReLU)

Introduced in 2000 by Teh & Hinton, the rectified linear unit (ReLU) has had a very rapid adoption over the past few years. Prior to the ReLU activation function, the hyperbolic tangent was generally accepted as the activation function of choice. Most current researches now recommend the ReLU for its superior training performances. As a result, most Neural Networks should utilize the ReLU on Hidden Layers and either softmax or linear on the Output Layer (Heaton, 2015). The following equation shows the very simple ReLU function:

$$y = \max(0, x) \qquad (3.5)$$

ReLU typically performs better than other activation functions for Hidden Layers. Part of the increased performance is due to the fact that the ReLU activation function is a linear, non-saturating function. Unlike the sigmoid/logistic or the hyperbolic tangent activation functions, ReLU does not saturate to -1, 0, or 1. A saturating activation function moves towards and eventually attains a value. The hyperbolic tangent function, for example,

saturates to -1 as x decreases and to 1 as x increases. Figure 3-8 shows the graph of the ReLU activation function:

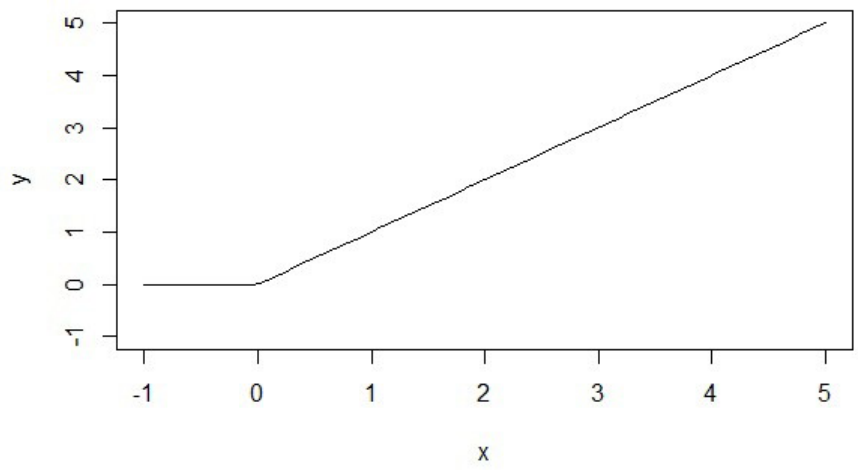

Figure 3-8 Rectified Linear Units (ReLU) (Heaton, 2015).

As it is shown in this paragraph, the best activation function for the Feed-Forward Network is the sigmoid function. Compared to the other activation functions presented, the sigmoid function has the following characteristics:

- non-linearity allows the representation of complex phenomena; unlike the linear function and the ReLu function, which are suitable for classification;
- small variations in the independent variable are associated with significant variations in the values of the dependent one, with respect to the hyperbolic tangent function;
- slowness in saturation unlike the step function.

3.2 Design and training Neural Network

The first step to design a new Neural Network consists in defining the application and the *experimental Dataset* to be used for the identification of both weights and biases. The application suggests to the designer the kind of network and the relative activation function to be selected. As for the other black-box models, the next step is to divide the data collected in two sets: the Dataset to be used in the identification of the model's parameters and the Dataset to be used in the validation of the designed model. Each item in a

Dataset is said *experimental point* (Spriet & Vansteenkiste, 1988) (Montgomery, 2013).

The number of parameters needed is evaluated by the following equation:

$$N_{par} = input * n_1 + n_1 + \sum_{i=2}^{k} (n_{i-1} * n_i + n_i) + n_k * output + output \quad (3.6)$$

Where:

- N_{par} is the number of parameters in terms of weight and bias to be identified;
- n_1 is the number of the neurons in the first Hidden Layer;
- n_i and n_{i-1} are the number of neurons in the *i-th* and *(i-1)-th* Hidden Layer respectively;
- k is the selected number of Hidden Layers;
- $input$ and $output$ is the cardinality of both input and Output Layers.

As it is shown in this equation, the number of parameters is directly correlated with the number of neurons and with the number of experimental points needed for the evaluation of weight and bias.

Once the number of neurons in the Hidden Layers have been selected, the evaluation of parameters (weights and biases) can start. This procedure is called training, because of its similarity to a biological network learning. The training can be supervised and unsupervised. Supervised training teaches the Neural Network to produce the ideal output. Unsupervised training usually teaches the Neural Network to place the input data into a number of groups defined by the Output Neuron count. In other words, the training function first minimizes the error on the output layer and then proceeds to the definition of weights and biases on the previous layers.Both supervised and unsupervised training are iterative processes.

For supervised training, each training iteration calculates how close the actual output is to the ideal output and expresses this closeness as an error percent. Each iteration, which is called epoch, modifies the internal weight matrices of the Neural Network to decrease the error rate to an acceptably low level.

Unsupervised training is also an iterative process. In this case the calculation of the error is not as easy, because there is not an expected output, that measures how far the unsupervised Neural Network is from ideal output. To avoid this problem, it is needed to iterate the training procedure for a fixed number of iterations and then try to use the network (Heaton, 2015).

In this work, supervised training has been used and the algorithm applied is the Levenberg-Marquardt Algorithm (LMA). Levenberg-Marquardt is a hybrid algorithm that is based on Gauss-Newton's method (GNA) and on gradient descent (backpropagation) (Marquardt, 1963) (Mozer, 1995) (Riedmiller & Braun, 1993). Thus, LMA combines the strengths of GNA with backpropagation. Although gradient descent is guaranteed to converge to a local minimum, it is slow. Newton's method is faster, but it often fails to converge. To improve the convergence, a hybrid method is built by using a damping factor to interpolate between the solutions achieved with both approaches.

The steps of this method are:

1. Calculate the first derivative of output of the Neural Network with respect to every weight.
2. Calculate the Hessian.
3. Calculate the gradients of the error (ESS) with respect to every weight.
4. Either set lambda to a low value (first iteration) or to the lambda of the previous iteration.
5. Save the weights of the Neural Network.
6. Calculate the delta weight based on the lambda, gradients, and Hessian.
7. Apply the deltas to the weights and evaluate the error.
8. If the error has improved, end the iteration.
9. If the error has not improved, increase lambda (up to a max lambda), restore the weights, and go back to step 6.

During the training of the network there are two phenomena that must be avoided: overtraining and overfitting.

The network goes in overtraining when the Dataset is too small, and it learns only the training events. Overfitting happens when the Set of training data is more detailed and the number of parameters to evaluate coincide with the information of the experimental point. In this case the Neural Network behaves like an interpolation curve. The two phenomena described can occur also when the error, in terms of mean square error, is too low, and number of training epoch is very high. (Patterson, 1999).

To avoid overtraining and overfitting, an early stopping technique has been implemented (Mastroberti & Pianese, 2000). This technique consists in dividing the experimental dataset in three sets (Figure 3-9):

- Training Set;
- Test Set;
- Validation Set.

At each epoch, the LMA algorithm is applied on the Training Set and the mean squared error is calculated on both test and Validation Sets. The network training stops when the mean squared error on the Test Set becomes constant

for a certain number of iterations or rapidly decreases from an epoch to the next one. The best Training Set is selected on the minimum value of the mean square error evaluated on the Validation Set (Marquardt, 1963).

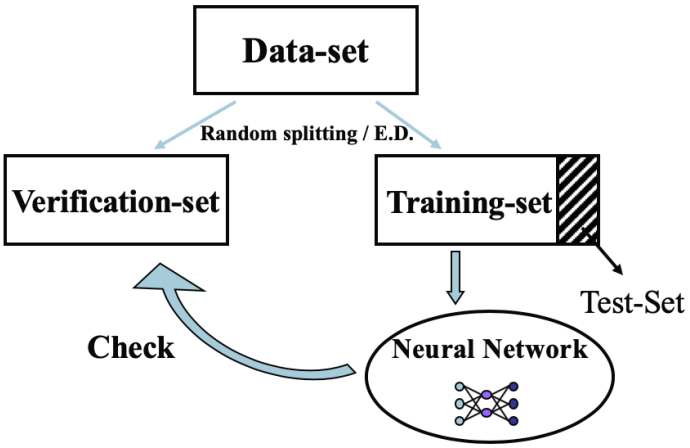

Figure 3-9 Scheme of Early-stopping technique (Mastroberti & Pianese, 2000).

CHAPTER 4
Application of Neural Networks to Diesel engine

This chapter reports the application of Artificial Neural Networks, to a Diesel Common Rail engine, for the calculation of :

- Specific fuel consumption (SFC);
- Mean Indicated Pressure (IMEP);
- Nitrogen oxides (NOx);
- Soot

4.1 Diesel engine and experimental environment description

The experimental data have been collected during previous experimental campaigns in the Energy and Propulsion Laboratory (eProLab) at the University of Salerno. In the engine test cell are located the engine test bed, auxiliary plants, sensors and emissions probes. The propulsion system is remotely controlled from an adjacent room, namely the control room, where are installed the order console and the main software for the management of hardware, actuators, and sensors. Figure 4-1 shows the engine test bench equipped with a light-duty engine EURO V FIAT F1A 2300 cm^3 Diesel Common-rail with VGT system, whose main technical data are reported in Table 4-1 (Arsie, et al., 2004) (Di Leo, 2015) (Tortora, 2017) (Rossomando, 2020)..

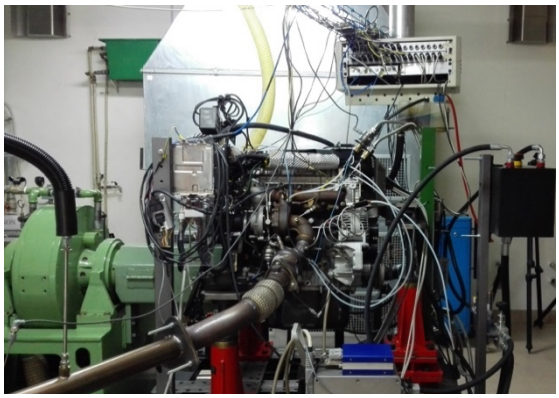

Figure 4-1 Engine test bench.

Table 4-1 Diesel engine characteristics

Diesel 2300 cm^3 CRi2 with VGT system	
Max Power [kW]	**107 @ 3600 rpm**
Max Torque [Nm]	**350 @ 1500 rpm**
N° cylinders	**4**
Displacement [cm^3]	**2287**
Compression ratio	**16.2**
Reference regulatory framework	**Euro V**

4.1.1 Engine test cell facilities

The engine test bench is composed by the seismic bench and the Eddy-Current dynamometric brake Borghi & Saveri FE200. In order to guarantee compliance with the safety regulations and the correct functioning of the engine, the following auxiliary systems are present::

- air introduction system;
- air drawing system;
- engine exhaust gas extraction system;
- cooling system;
- fuel supply system.

The cooling plant, besides the dynamometer brake, is used for engine water and oil cooling too. The plant consists of two heat exchangers for the engine cooling (water and oil), a branch for the brake cooling and a evaporative

cooling tower located outside the laboratory. An independent electric fan is used to cool the engine intercooler with fresh air.

Concerning the fuel supply system, a fuel tank of 250 l is located outside the laboratory and a pump close to the tank supplies the fuel to the laboratory. Before reaching the engine, the fuel flow is processed by a gravimetric fuel balance (AVL 733S Dynamic Fuel Meter, Figure 4-2) for the fuel consumption measurement.

Figure 4-2 AVL 733S Dynamic Fuel Meter.

The engine is equipped with the sensors and measurement instruments described in Table 4-2, with the corresponding accuracy.

Besides the engine's own flow meter, managed by the ECU, an ABB Sensyflow FMT700-P air-flow meter is also used to achieve higher measurement accuracy. It is shown in Figure 4-3 and it operates according to the principle of the hot-film anemometer.

Table 4-2 Sensors accuracy

Measurement	Sensor type	Accuracy
In-cylinder pressure [KPa]	Piezo-electric	± 0.2 %
Air mass flow [Kg/h]	Hot-wire	± 1%
Fuel mass flow [Kg/h]	Gravimetric	±0.12%
Temperature(≥350°C)	Thermocouples	±5 °C
Temperature(<350°C)	Resistance	±1.5°C
Intake pressure	Piezo-resistive	±0.05%
Turbo-speed	Eddy current	±0.05%
CO [%vol]	Infrared	±0.5%
CO_2 [%vol]	Infrared	±0.5%
O_2 [%vol]	Paramagnetic	±0.05%
NO_x [ppm]	Ceramic sensor	±10%
Soot [mg/m^3]	Smoke meter	±6%

Figure 4-3 Flowmeter Sensyflow.

The crank angle position and the engine speed are evaluated using an optical encoder. Maximum resolution is 0.2 degrees and zero degrees is assumed to be the Top Dead Center (TDC) during compression. This last one is called the "sync point", so the full pressure cycle (720 degrees) covers the range from -360 up to 359.8 degrees. The pressure inside the cylinder is measured, in a single cylinder, by a piezoelectric transducer placed in a glow plug adapter, with sensitivity equal to 16 pc/bar. The signal pegging was performed by applying the thermodynamic zero level correction method,

based on the assumption of a constant polytrophic coefficient along the compression stroke.

Turbo engine speed is measured using a micro-epsilon system. A very fast proximity sensor responds to the passage of the turbocharger blades (depending on the initial state) made with electrically conductive materials. The principle of Eddy-Current leakage influences impedance changes in a measuring coil (sensor). This impedance change gives rise to an electrical signal. Engine NO_x emissions are measured by the NGK/Continental intelligent NO_x sensor (Figure 4-4) located upstream of the turbine. It consists of three main parts: the sensor body, the control module and the transmission wiring. The sensor body is made of Zirconium Oxide (ZrO_2) with an integrated heater, two cavities and three oxygen pumps. The heater is integrated in the sensor body to raise the temperature from a minimum of 80°C to a maximum of 120°C. After the oxygen concentration drops to a predetermined level in the first cavity, the NO_x-reducing catalytic activity takes place in the second cavity and the generated oxygen is detected as oxygen pumping flow, which is proportional to the NO_x concentration. The intelligent NO_x sensor control module communicates with the engine control module via Controller Area Network (CAN) protocol.

Figure 4-4 Continental NO_x sensor.

Soot emission measurement is performed by the AVL Smoke Meter 415S. The measured value (filter blackening number) corresponds to the black Soot content in the engine emission. The exhaust is sampled from the exhaust pipe at a defined flow rate and passed through clean filter paper in the instrument. The filtered particles cause the blackening on the filter paper which is detected by a photoelectric measuring head and evaluated in the microprocessor to produce the result in FSN (Filter Smoke Number). This value is converted in a concentration value, expressed in $\frac{mg}{m^3}$, through an expression provided by AVL. The Smoke Meter communicates with the test cell computer via AK protocol using the RS 232 serial interface.

Specific gas analysers are used to measure the main engine emissions: HC, CO, CO_2, O_2. The box with all dedicated modules is shown in Figure 4-5.

Figure 4-5 Gas analyzer box. On the left side the sampling pump, on the right side the control module (Advance Optima) and the different gas modules.

All modules are provided by ABB. Hydrocarbons (HC) emissions are measured by a Flame Ionization Detector (FID), using a continuous diffusion flame of external combustion air O and burnable gas H_2. The Uras 14, an infrared (NDIR) gas analyser, is used to measure CO and CO_2 emissions and the thermomagnetic principle is used for the selective detection of oxygen by means of Magnos 106. The AVL Pre-Filter HSS i60 is also used to filter particles from engine exhaust, in combination with an exhaust measurement system, in order to protect the components in the exhaust measurement system against contamination and to guarantee the measurement quality in the long run.

The AVL Pre-Filter is shown in Figure III.5, it is placed between the engine exhaust line and the gas analysers, linked to both systems by means of heated cables, in order to prevent the gases condensation. An analysers-dedicated pump draws the sampling gases from the exhaust line, because of this configuration the pump forces gases to pass across the ceramic filter before reaching the gas analysers.

Figure 4-6 Pre-Filter AVL HSS-i60.

A more accurate measurement of NO_x emissions is performed by the Cambustion CLD500 fast NO_x sensor that is used to detect the NO and NO_x concentration across the DPF. The instrument is a Chemi-Luminescence Detector (CLD) used for measuring the NO and/or NO_x concentration in a sample gas with a very fast response time. The reaction between NOx and O_3 (Ozone) emits light; this reaction is the basis for the CLD in which the photons produced are detected by a photo multiplier tube. The CLD output voltage is proportional to NO_x concentration. The light-producing reaction is very rapid so careful sample handling is important in a very rapid response instrument. This is achieved by locating the detectors in remote sample heads which are positioned very close to the sample point in the engine and conveying the sample gas to the detectors under the influence of a vacuum through narrow heated capillaries. This method minimises the mixing of the sample prior to its entry to the detector.

4.1.2 Systems for the test bench management

The control between the engine and the dynamometric brake is performed by means of an integrated hardware and software lay-out of the engine test stand. The main hardware systems are:

- the AVL microIFEM for the management of engine-dyno interaction by test bench sensors and actuators;
- the AVL Indimicro to monitor and process the indicating data;
- the control unit ETAS ES592.1 to manage the Engine Control Unit (ECU).

The corresponding software to manage the aforementioned hardware are:

- AVL Puma Open;
- AVL IndiCom
- ETAS Inca.

In Figure 4-7 is presented the command position with a direct overlook on the engine test cell. The three screens in the figure show the different user-interface related to Puma, IndiCom and Inca from the left to the right respectively.

Figure 4-7 Engine control console.

The setting and control of the AVL test bench is performed via the AVL EMCON (EMission CONtrol) panel. In addition, the AVL test bench has a throttle actuator as well as a system cabinet containing a complex wiring to connect hardware and software devices and to monitor the system during operation. Furthermore, it represents the interface between the measurement devices and the master software AVL Puma Open.

AVL Puma Open represents the interface between the user and the cable-connected measuring devices, as well as the test bench. By means of the control console, three main driving variables can be managed (and monitored on Puma Open) to define the engine working condition:

- brake torque;
- engine load;
- and engine speed.

An operating engine point is determined by fixing only two driving variables depending on the application.

Generally, in the experimental activity, the motor speed and load are managed to define the operating point of the motor. Puma Open also allows you to configure and monitor various software programs/test equipment such as INCA, IndiCom and the exhaust gas analyser. The pre-set limitations for the measured parameters are checked and interventions are carried out if necessary; on the contrary, the cooling temperature is controlled directly by Puma Open.

Measured data from smoke, fuel mass flow, high and low pressure sensors are collected and can be exchanged with INCA.

Furthermore, the display and storage of the measurement data available in both graphical and tabular form enables supervision and subsequent evaluation.

The AVL IndiCom interface allows to instantly monitor the pressure cycle within the cylinder. Although AVL Indimicro has 4 input channels, only one is dedicated to the pressure inside the cylinder; while two channels are dedicated to the pressure upstream and downstream of the turbine and the last channel is dedicated to the analog output of the Lambda Meter for measuring O_2 in suction.

Among others, IndiCom post-processes the pressure inside the cylinder in real time, providing combustion-related variables such as:

- Indicated Mean Effective Pressure (IMEP);
- Heat Release Rate (HRR);
- Mass Fraction Burned Angles (MFBX, i.e. X generic mass fraction burnt);
- Combustion Noise (CN).

ETAS INCA v7.0 is used to capture, visualize, record and evaluate measuring signals from the Electronic Control Unit (ECU MJD8F3.SVI), provided by Marelli.

It is directly interfaced with the ECU by means of the control unit ETAS ES592.1 as indicated in the scheme of Figure 4-8.

Thanks of this link, engine operating modes different from the basic calibration can be easily proceeded. It is possible to handle the main combustion control and measured variable such as rail pressure, start of injection, boost pressure, EGR valve opening etc., with the aim to find out the optimal calibration. Definitely, in Figure 4-8 blue line refers to the actuation track: the engine control variables are set in Inca and actuated to the engine by means of the ECU; on the other hand, the red line refers to the feedback on control strategies from the engine.

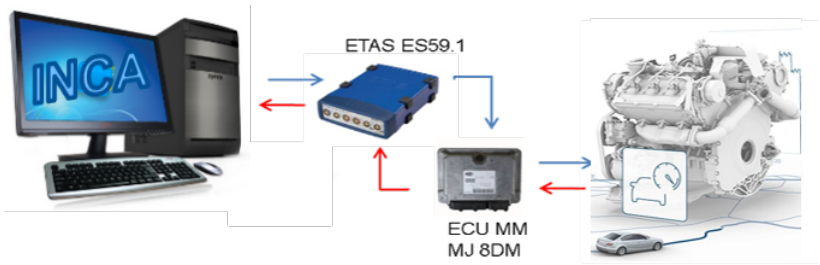

Figure 4-8 Communication scheme between user and engine. Actuation line in blue: input engine variables set by the user; Acquisition line in red: feedback on control strategies from the engine.

4.2 Preliminary results.

Neural Networks are applied to the control variable of a Diesel Engine in order to evaluate the Specific Fuel Consumption (SFC). For the design, the training and the validation of Neural Networks the “MATLAB Deep Learning ToolBox” is used.

The experimental data were collected during previous experimental campaigns conducted at the eProLab laboratory with the experimental

equipment described in paragraph 4.1, on the Diesel engine described in Table 4-1 (Arsie, et al., 2004) (Di Leo, 2015) (Tortora, 2017) (Rossomando, 2020).

Before designing the Neural Network, the variables to be given as input at the network must be chosen. Since the Specific Fuel consumption depends directly by the quantity of fuel injected and by the thermodynamic cycle, the variables selected as input are:

- $speed$ in rpm, that identify the operative point of the engine;
- EGR ratio, that influences the temperature of the air mixture inside the cylinder;
- SOI_{MAIN} in $deg\ BTDC$, the time when the main injection starts;
- Q_{ref} in $\frac{mm^3}{stroke}$, the total amount of fuel injected in all injections.

Then the Neural Network considered is a Feed-Forward Network with four inputs and one output; since the Dataset is composed by 73 experimental points, the number of Hidden Layers is fixed to one. The maximum number of neurons in the Hidden Layer is obtained by the following relationship:

$$N_{neuron\_max} = \frac{N_{point} - 1}{input + 2} \quad (4.1)$$

Networks are trained with the Levenberg-Marquardt Algorithm.
The networks are evaluated by calculating the correlation coefficient R^2as follows:

$$R^2 = 1 - \frac{\sum_i (y_i - f_i)^2}{\sum_i (y_i - \bar{y})^2} \quad (4.2)$$

Where:

- y_i is the measured value;
- $\bar{y}$ is the mean of measured values;
- f_i is the value calculated by the Neural Network.

For the first test we consider a random division of the 73 experimental points:

- 51 for the Training Set;
- 11 for the Test Set;
- 11 for the Validation Set.

Then, according to (4.1), the maximum number of neurons is 8.

Table 4-3 shows that, as expected, the network with the best value of the correlation coefficient is that with 8 neurons in the Hidden Layer.

Table 4-3 Results for the first experiment

Number Hidden Neurons	5	6	7	8
Epochs	14	12	13	16
$\boldsymbol{R^2}$	0,9607	0,9691	0,859	0,9784

The Figure 4-9 shows the plot of the measured vs calculated data; the net gives different results in correspondence of the value of SFC equal to $220\,\frac{g}{KWh}$.

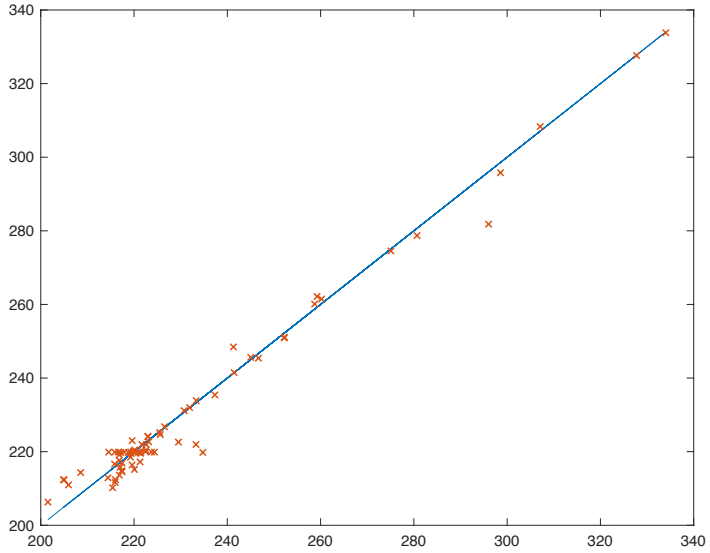

Figure 4-9. Plot of measured vs calculated data of the specific fuel consumption for 73 experimental operating conditions simulated by the Neural Network with 8 neurons in the Hidden Layer.

In the second test the same Dataset is used as before; and the experimental points are randomly divided in the following way:

- 47 for the Training Set;
- 7 for the Test Set;
- 7 for the Validation Set.

The remaining 12 points are used as inputs to the Artificial Neural Networks used to verify their generalizability.

The maximum number of Hidden Neurons is 7.

Table 4-4 shows that the best value for the correlation coefficient of the training procedure is obtained by the network with 5 neurons in the Hidden

Layer, but with the manual validation the best performance is obtained with 6 neurons in the Hidden Layer. The network with 7 neurons in the Hidden Layer shows a mean R^2 performance both in case of automatic and in case of 12 Point Validation.

Also in this test the network with 7 neurons in the Hidden Layer shows the same behavior of the previous test around the points that exhibit a value of SFC of $220\frac{g}{KWh}$ (Figure 4-10 and Figure 4-11).

Table 4-4 Results for the second experiment.

Number of neurons	5	6	7
Epochs	16	18	9
R^2 (training)	0,9743	0,9439	0,9652
R^2 (12 Point Validation)	0,9616	0,9759	0,9647

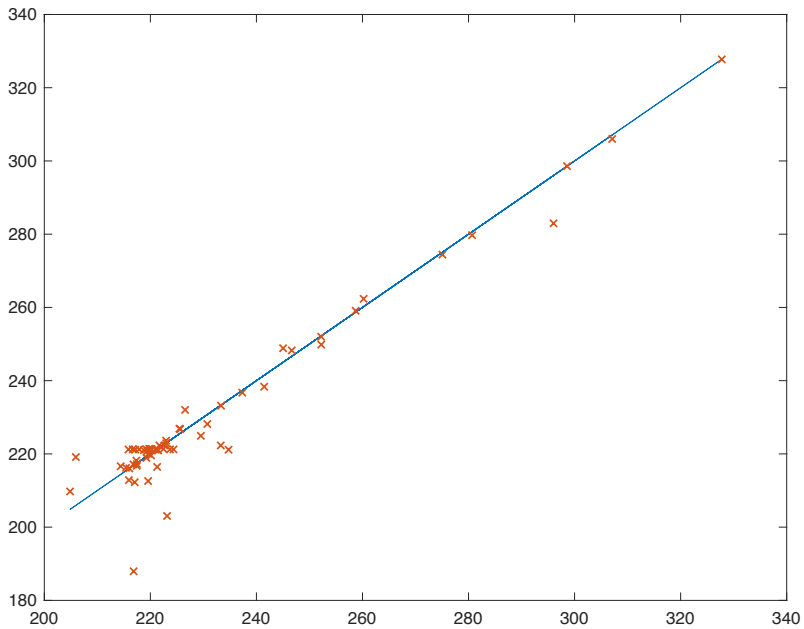

Figure 4-10 Plot of measured vs calculated data of the Neural Network with 7 neurons in the Hidden Layer.

.

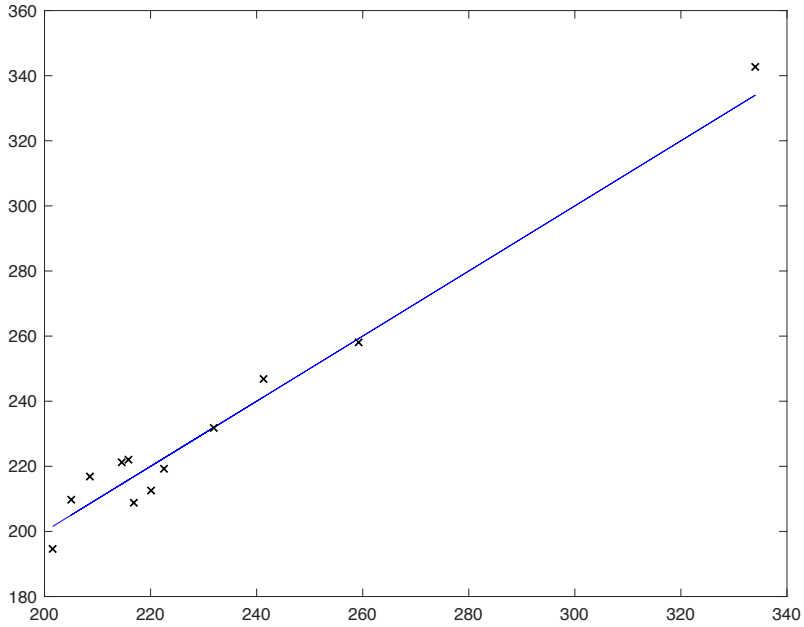

Figure 4-11 Plot of measured vs calculated data by the network with 7 neurons for the 12 validation points as input.

This behavior suggests the need of an analysis of the input data whose results are shown in the following figures (from Figure 4-12 to Figure 4-16).

Figure 4-12 shows 33 points between 1400 and 1500 rpm and no data in the ranges of 1500-1700 rpm, 2000-2300 rpm, and 2400-2600 rpm.

In Figure 4-13, 70 out of 72 SOImain points are contained in a range between -2 and 8 degBTDC, of which 45 in the typical injection range of the main (2.5-5 degBTDC).

Figure 4-14 and Figure 4-15 show a homogeneous distribution of the values of EGR and Qref respectively, while Figure 4-16 shows the presence of 43 points for SFC values between 210 and 220 g/kWh.

In the histograms of Figures from 4-12 to 4-16 it is shown that the experimental data, although representative of all operative plan of the Diesel engine, are not homogenous with respect to the considered variables for network training.

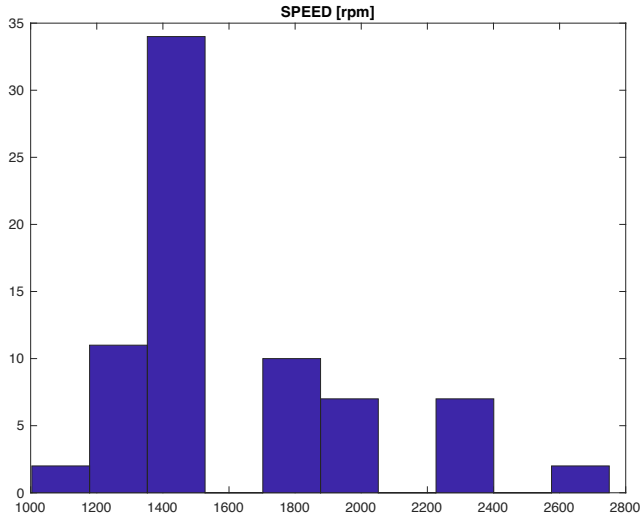

Figure 4-12 Distribution of speed data.

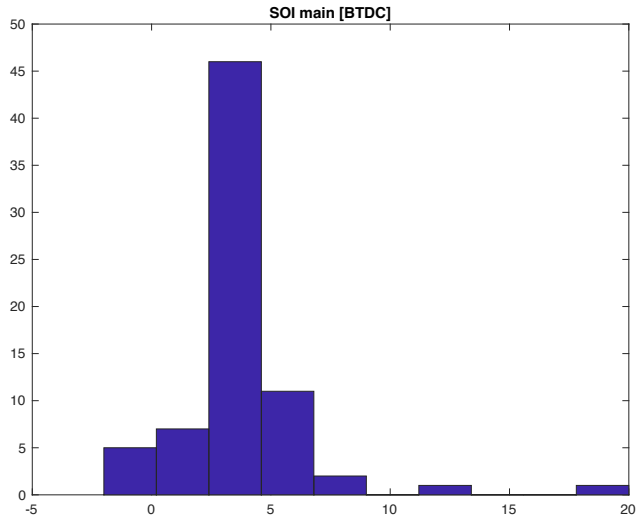

Figure 4-13 Distribution of SOI_{main} data.

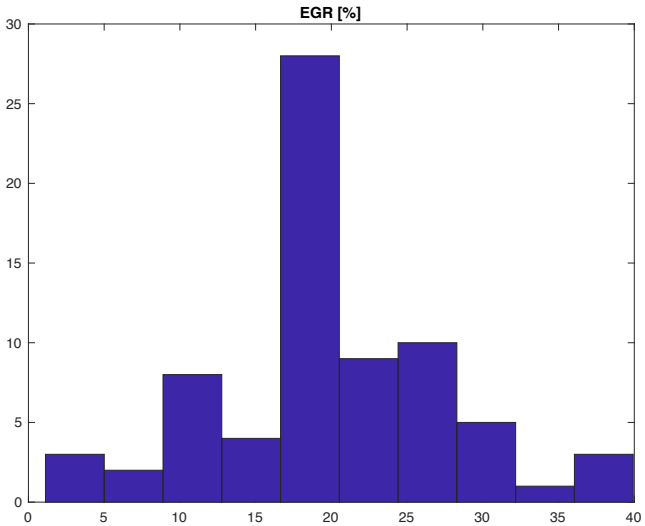

Figure 4-14 Distribution of EGR data.

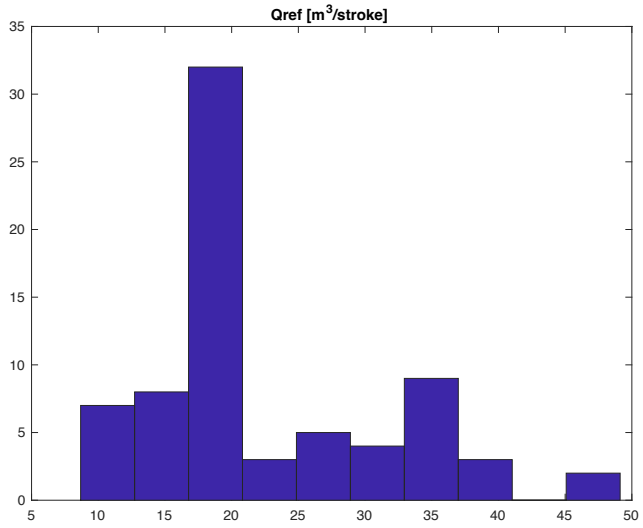

Figure 4-15 Distribution of Q_{ref} data.

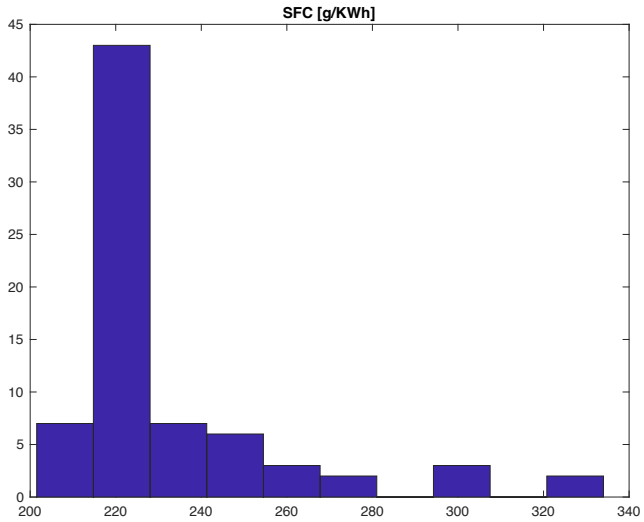

Figure 4-16 Distribution of SFC data.

4.3 The Entire Experimental Dataset and correlation analysis

On the same engine described in the previous paragraph a new set of data was collected and is representative of the entire operating plan of the engine (speed and torque).

The Dataset is composed of 282 experimental points and it has been divided in the following sets for the Early-stopping technique:

- 75% (202 points) for the Training Set;
- 15% (40 points) for the Validation Set;
- 15% (40 points) for the Test Set.

It was processed to remove the outliers for which the following procedure was followed:

1. Data collection;
2. Verification of the consistency of the measurements of the physical quantities considered;
3. For each of the quantities considered, the following steps were followed:
    a. Subdivision of the measures into clusters, based on the density of the points;
    b. Identification of mean and standard deviation for each cluster;
    c. Definition of the acceptance interval using the mean value of the standard deviations on all clusters;

   d. Identification of points with a standard deviation higher than the value account;
4. Detection of 0 with measurement errors;
5. Removal of the points identified in points 4 and 3.d.

The entire operation plan and the results of the described procedure are shown in Figure 4-17.

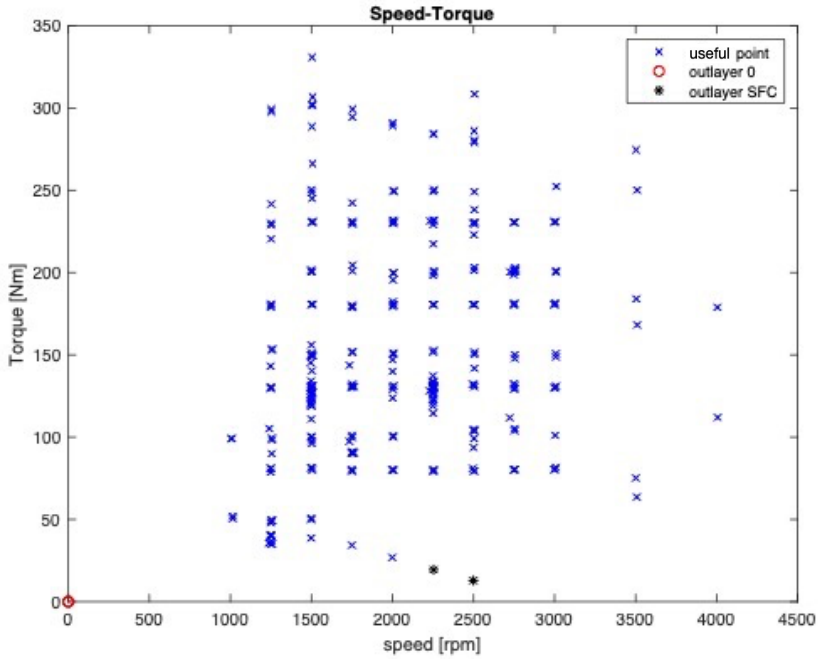

Figure 4-17 Representation of the engine operative plan with outliers

As shown in Figure 4-18, the points in terms of speed are homogeneous between 1000 and 3000 rpm with peaks at 1500 and about 2300 rpm. There are few representative points at high speed (3000-4000 rpm).

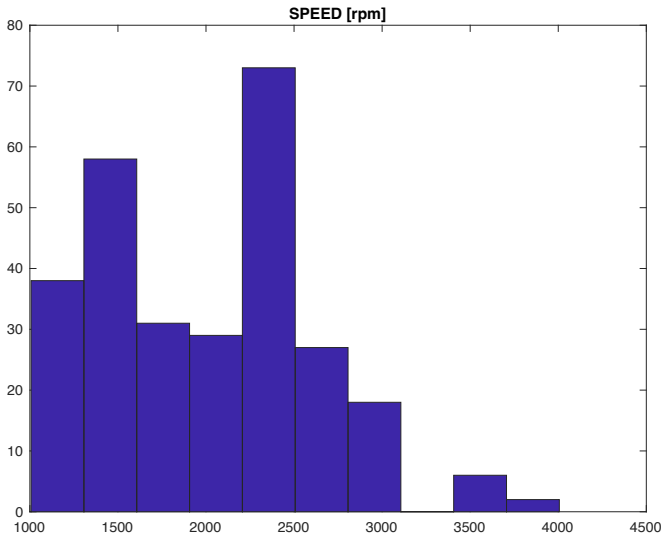

Figure 4-18 Distribution of speed.

The data for the torque covers the entire operating range quite well with peaks of around 130 and 200 Nm (Figure 4-19).

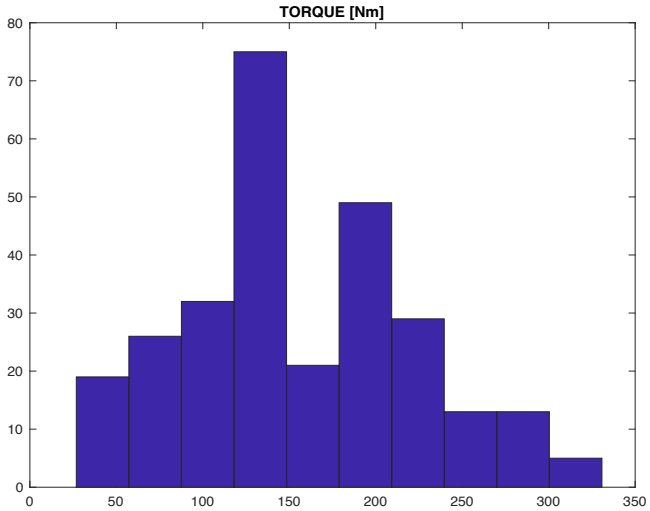

Figure 4-19 Distribution of Torque.

Almost half of the experimental points show a thickening around 0% of EGR since those points derive from experimental studies on nitrox oxide formation (**Figure 4-20**).

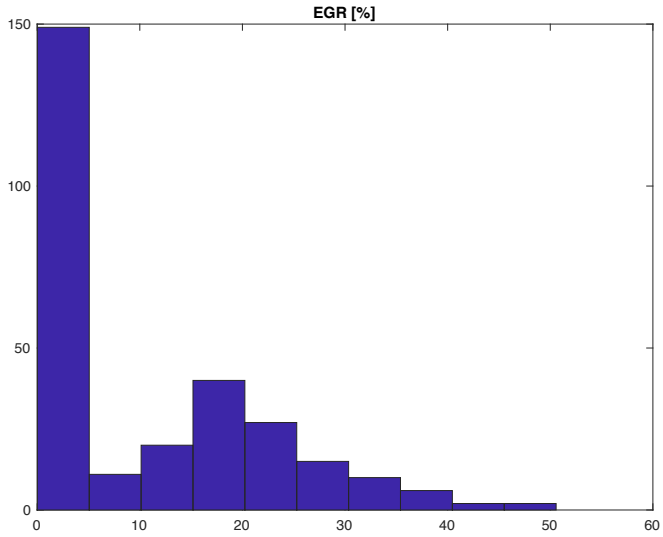

Figure 4-20 Distribution of EGR

To avoid misfiring and obtain optimal combustion, most of the experiments were conducted with main injections between 0 and 10 degrees before the top dead center as shown in Figure 4-21.

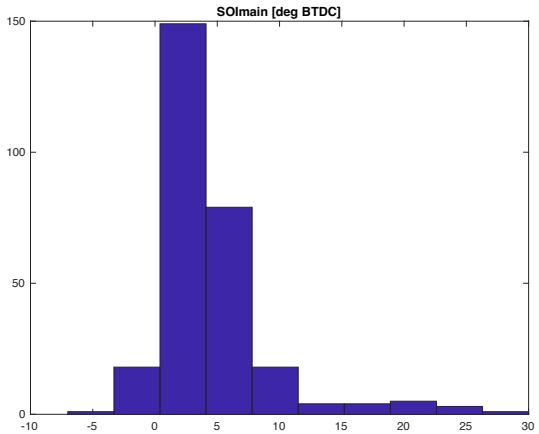

Figure 4-21 Distribution of SOI_{main}

As regards the fuel injected, there are less than 10 points from 60 to 65$\frac{mm^3}{str}$ (Figure 4-22).

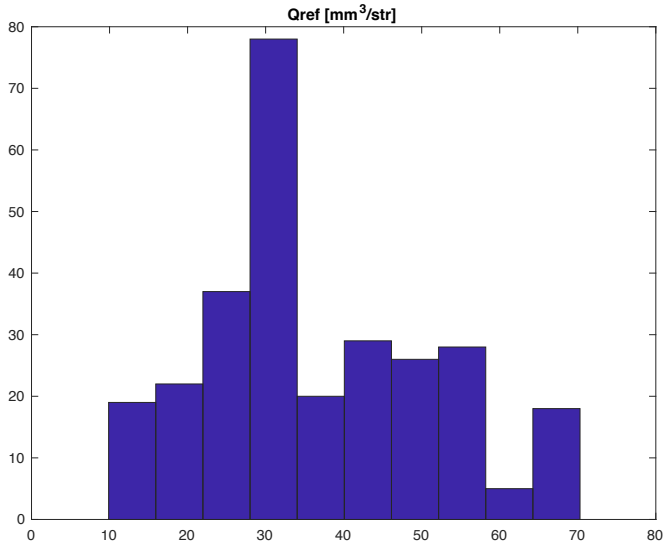

Figure 4-22 Distribution of total quantity of fuel injected per cycle

Some values of rail pressure are at high pressure since they were used to study the effect on generation of particulate matter (Figure 4-23).

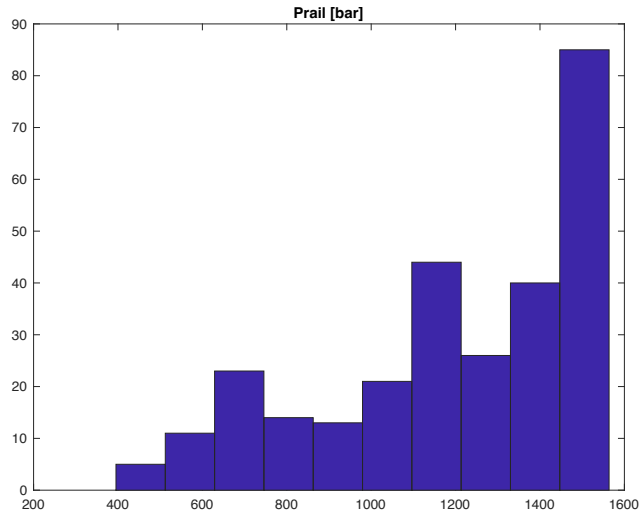

Figure 4-23 Distribution of rail pressure

In order to consider the use of the operating variables in the input pattern of Neural Network, a correlation analysis (Montgomery, 2013) was performed as shown in Table 4-5:

Table 4-5 Analysis on the correlation among control and operating engine variables.

	VGT	M_{AIR}	AFR	EGR	O_2	P_{BOOST_ABS}	P_{MAN}
VGT	1,0000	-0,8468	0,0084	0,2622	-0,1172	**-0,7387**	-0,7355
M_{AIR}	-0,8468	1,0000	-0,0106	**-0,4260**	0,0956	0,9562	0,9544
AFR	0,0084	-0,0106	1,0000	-0,2009	0,9312	-0,1885	-0,1920
EGR	0,2622	**-0,4260**	-0,2009	1,0000	-0,1860	-0,3841	-0,3827
O_2	-0,1172	0,0956	0,9312	-0,1860	1,0000	-0,1074	-0,1121
P_{BOOST_ABS}	**-0,7387**	0,9562	-0,1885	-0,3841	-0,1074	1,0000	**1,0000**
P_{MAN}	-0,7355	0,9544	-0,1920	-0,3827	-0,1121	**1,0000**	1,0000

The correlation coefficients in the table asses the mathematical link among control and operating engine variables: for a value close to 1, the variables concerned have almost the same behavior (i.e., are linked), whereas if the value is 0 the variables are independent from each other. Plus and minus signs indicate a direct or an inverse link between the two variables analysed, respectively. The analysis performed suggests to consider an input pattern with VGT and EGR, that are actuated (i.e., controlled) variables, and another pattern with the air flow in the inlet circuit (Mair) and the pressure in the manifold, i.e. the control volume near inlet valve. Manifold pressure can be evaluated as equal to Pboost or Pman, that have almost the same values, as it can be observed in the table.

The same procedure is applied to evaluate the distribution in frequency of the output of each network.

The Specific Fuel Consumption has a variation of about 80 g/KWh in the entire operative plan; the points that could appear as outliers are in the region where there are high values of speed and torque (Figure 4-24).

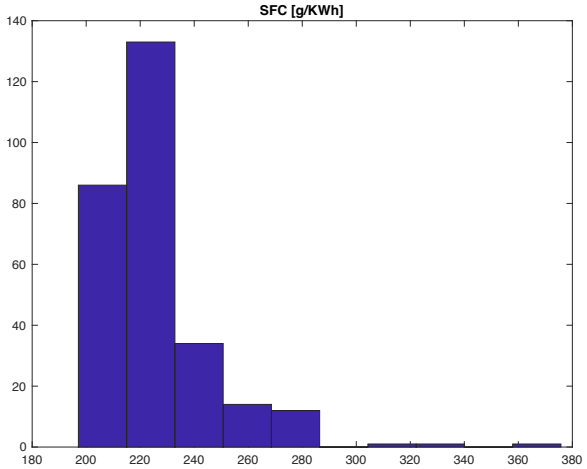

Figure 4-24 Distribution of Specific Fuel Consumption.

Indicated Mean Pressure Data are representative of the entire operative plan (Figure 4-25).

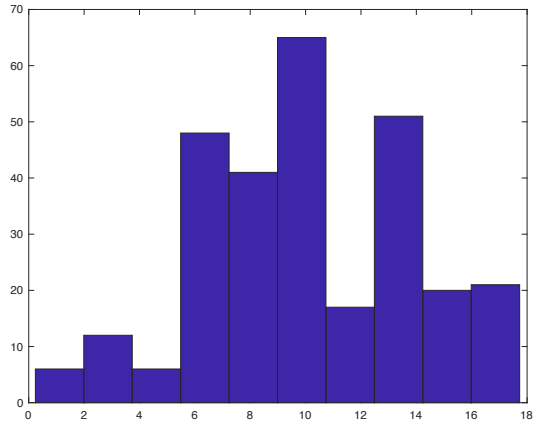

Figure 4-25 Distribution of Indicated Mean Pressure (IMEP) in bar

From Figure 4-26, it is possible to notice the effects of the combined control of both rail pressure and SOI_{main} on the emissions of NOx; indeed, that action determines emission levels that are lower with respect to those expected in the operating points with 0% of EGR.

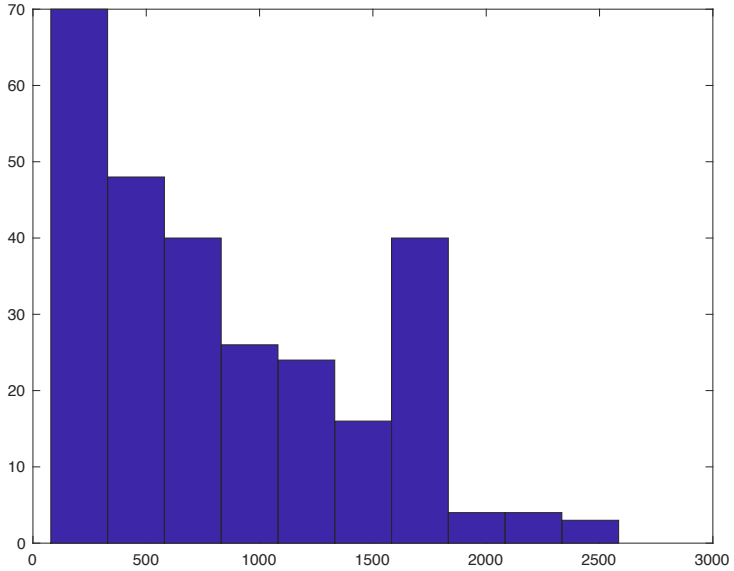

Figure 4-26 Distribution of Nitrogen Oxides (NO_X) in part of million (ppm).

During one experimental campaign some problems occurred in the acquisition toolchain; therefore, the number of experimental points with information about soot is the lowest of the entire Dataset (Figure 4-27).

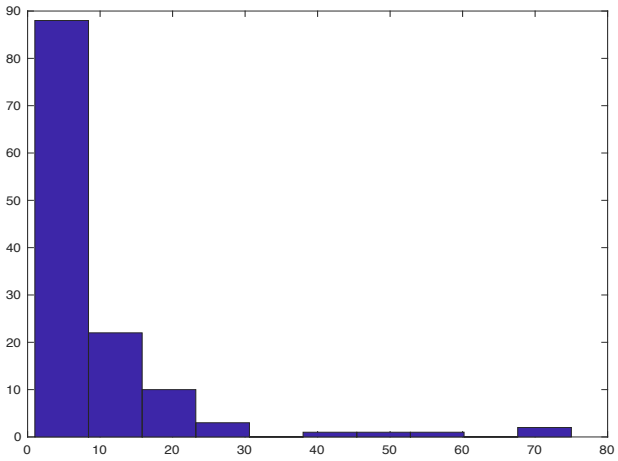

Figure 4-27 Distribution of soot in mg/m^3.

4.4 Training and validation of the Neural Networks

The experimental Dataset and the relative analysis described in the previous paragraph are applied in this section with the aim to obtain the Artificial Neural Networks, according to the following procedure:

1. Train the network with early-stopping techniques to find the optimal cardinality of the three subsets (train, validation, test) built from the entire experimental database.
2. Train the network by varying the initial value of weight and bias with the optimal subsets division found in step 1.

During each step, 10^4 networks have been analysed and the optimal one has been selected using as evaluation parameter the correlation coefficient on all the experimental Dataset, to guarantee precision and generalizability.

The different initial values of weight and bias are selected randomly in a normalized Gaussian distribution where the standard deviation has been calculated with the following formula:

$$\sigma = \sqrt{\frac{2}{n_{in} + n_{out}}} \qquad (4.3)$$

where n_{in} represents the dimension of the input pattern and n_{out} represent the dimension of the output one.

In this work, the Neural Networks have been implemented with a dimension of output pattern equal to 1. In fact, for each input pattern, four networks have been developed to calculate SFC, IMEP, NO_X and soot. In the Figure 4-20, Figure 4-21 and Figure 4-22 are sketched the networks with 3 different input patterns.

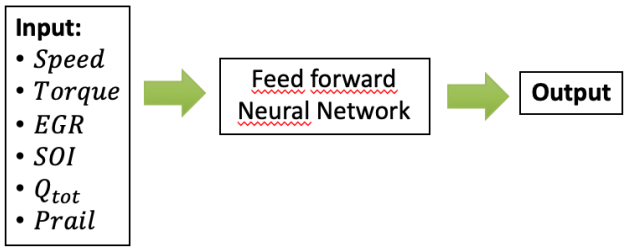

Figure 4-28 Input pattern #1

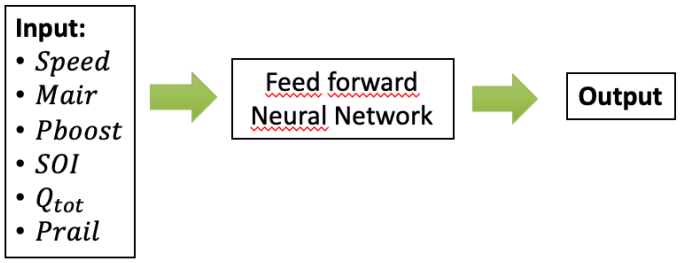

Figure 4-29 Input pattern #2

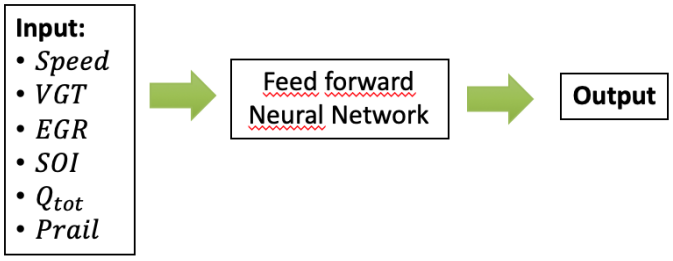

Figure 4-30 Input pattern #3

The first input pattern (fig. 4-20) is used only to improve the efficiency of the Neural Network and to test how the network can describe phenomena with the considered experimental Dataset. In fact, specific fuel consumption can be calculated directly from Q_{tot}, speed and torque.

In the second pattern (fig 4-21) the input variables are selected as a mix of the state variables (speed), the actuating variables (SOI, Q_{tot} and P_{rail}) and the inlet measured variables (M_{air} and P_{boost}):

In the third pattern (figure 4-22) there are only state and actuating variables.

4.5 Discussion

This section reports the analysis of the results for the training and validation of the Neural Networks described in the previous paragraph.

In Table 4-6 and Table 4-7 are summarized the results via correlation coefficient (R^2) and statistical indicators of the training of the Neural Networks both using early stopping techniques (Table 4-6) and by varying the weight and bias initial values (Table 4-7) (Mastroberti & Pianese, 2000).

For each structure built by varying the number of neurons in the Hidden Layer 10^4 Neural Networks have been trained, saving the correlation coefficients and the statistical data; thus storing all information on precision and generalizability. After that, the minimum, the maximum, the arithmetic mean, mode, median and standard deviation have been evaluated to study the distribution of the correlation coefficients.

From this analysis, the Neural Network that appears to be the optimal one is the one with 13 neurons in the Hidden Layer. As regards the calculus of specific fuel consumption, networks show a good correlation coefficient that is about 0,99. The same analysis was done for all networks and all schemes, in terms of input patterns and output, as previously described this has led to the same satisfactory conclusions.

Table 4-6 Correlation coefficient and statistical indicators of Neural Networks implemented with data pattern #1 with Early-stopping techniques.

Number neurons of hidden Layer	6	7	8	9	10	11	12	13	14	15	20	25
Epoch	75	32	46	45	26	63	28	36	34	26	29	43
Best epoch	69	26	40	39	20	57	22	30	28	20	23	37
Max R^2	0,9814	0,9822	0,9835	0,9836	0,9832	0,9856	0,9839	0,9861	0,9853	0,9851	0,9872	0,9851
Mean R^2	0,9485	0,9503	0,9516	0,9512	0,9523	0,9519	0,9532	0,9534	0,9523	0,9524	0,9494	0,9467
Min R^2	0,0000	0,0045	0,0011	0,0002	0,0004	0,0000	0,0042	0,0087	0,0446	0,0043	0,0001	0,0362
Relative variation	0,9814	0,9778	0,9823	0,9835	0,9828	0,9856	0,9797	0,9774	0,9407	0,9808	0,9870	0,9489
Percentage relative variation	100,00	99,55	99,88	99,98	99,96	100,00	99,58	99,12	95,47	99,57	99,99	96,33
Mode	0,9662	0,9644	0,9759	0,9669	0,9474	0,9645	0,9672	0,9504	0,9776	0,9733	0,9701	0,9514
Median	0,9619	0,9633	0,9643	0,9649	0,9653	0,9654	0,9658	0,9656	0,9656	0,9651	0,9634	0,9600
Variance	0,0032	0,0032	0,0031	0,0035	0,0031	0,0035	0,0026	0,0024	0,0030	0,0025	0,0032	0,0027

Table 4-7 Correlation coefficient and statistical indicators of Neural Networks implemented with data pattern #1 varying weight and bias initial values

Number of neurons of the Hidden Layer	6	7	8	9	10	11	12	13	14	15	20	25
Epoch	56	192	120	107	35	46	38	65	33	21	33	43
Best epoch	50	186	114	101	29	40	32	59	27	15	27	37
Max R^2	0,9818	0,9831	0,9848	0,9827	0,9824	0,9853	0,9847	0,9869	0,9874	0,9817	0,9850	0,9860
Mean R^2	0,9434	0,9702	0,9634	0,9632	0,9650	0,9606	0,9711	0,9680	0,9783	0,9555	0,9674	0,9703
Min R^2	0,2217	0,3274	0,0107	0,0028	0,0860	0,2099	0,5346	0,0222	0,0003	0,0184	0,2860	0,6912
Relative variation	0,7601	0,6558	0,9741	0,9799	0,8963	0,7754	0,4502	0,9648	0,9871	0,9633	0,6991	0,2948
Percentage relative variation	77,42	66,70	98,92	99,71	91,24	78,69	45,72	97,75	99,97	98,13	70,97	29,89
Mode	0,9780	0,9738	0,9531	0,9718	0,9771	0,9736	0,9731	0,9460	0,9837	0,9599	0,9817	0,9705
Median	0,9674	0,9758	0,9714	0,9693	0,9702	0,9655	0,9768	0,9783	0,9800	0,9595	0,9724	0,9735
Variance	0,0022	0,0003	0,0007	0,0009	0,0006	0,0005	0,0002	0,0007	0,0002	0,0007	0,0003	0,0002

The only model that has shown results with lower precision is the one that calculates the soot. In fact, the maximum value of the correlation coefficient is about 0.97.

A detailed graphic representation is reported from Figure 4-31 to Figure 4-34 with a comparison between measured and simulated data.

Figure 4-31 compares the results for the simulation of soot performed with the best Neural Network with 13 neurons in the Hidden Layer by using input pattern #2 (Figure 4-29). The figure shows the distribution of the values calculated by the model with respect to those measured, both on the Test Set and in the entire experimental plan. It is worth noting that there are many points gathered around the value 0. For the same variable, Figure 4-32 shows the distribution of the relative percentage error with respect to the experimental measurements for each point. The error ranges from about -200% error to about 500% with about 80% of data within an error less than ±50%. This result is conditioned by the size of the Dataset of available experimental data which is equal to 128, since on a small number of data the propagation of the error increases in the intervals where they are more scattered. Moreover, the presence of many points close to 0 is justified by the fact that in the Dataset there are many points with low percentages of EGR (0-5%) and, therefore, there are two effects:

- the particles are easily oxidized in the combustion chamber;
- the number of particles formed in previous cycles is negligible because of the very low EGR.

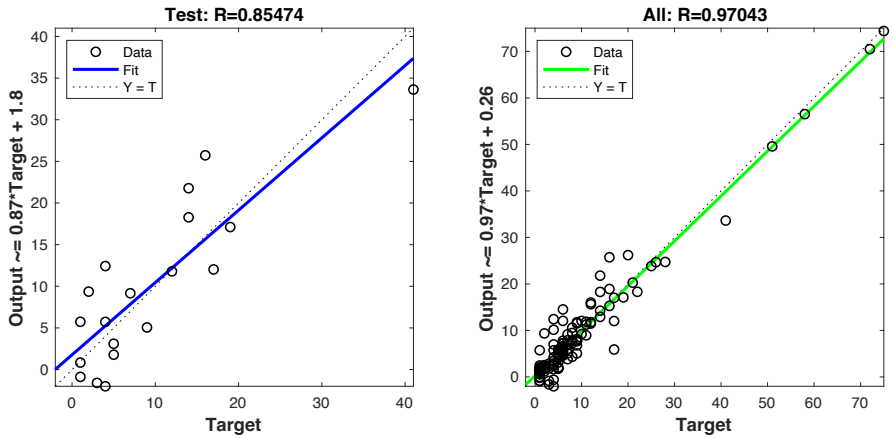

Figure 4-31 Results for the best Neural Network, with 13 neurons in the Hidden Layer, for calculus of soot by using input pattern #2 (Figure 4-29): on the left, the measured vs calculated data on the Test Set; on the right, the measured vs calculated data on all experimental points

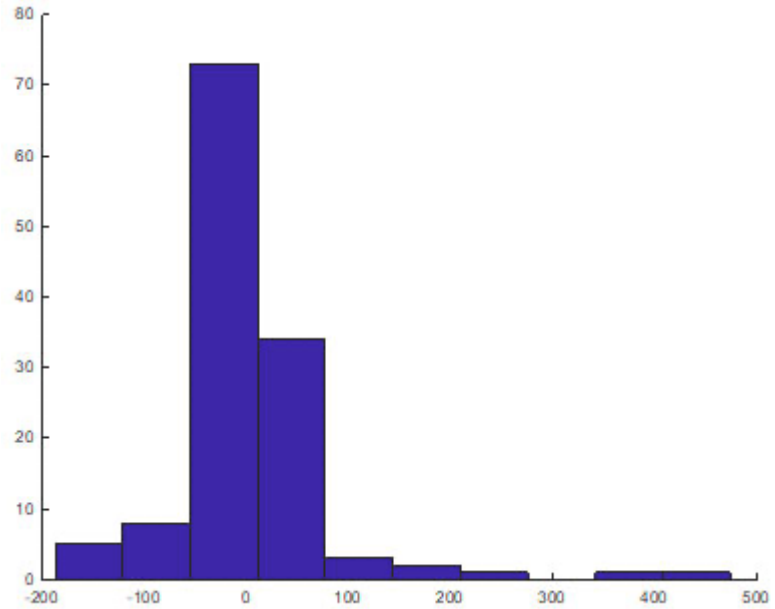

Figure 4-32 Distribution of error percentage of best Neural Networks for calculus of soot with 13 neurons in the Hidden Layer by using input pattern #2 (Figure 4-29). On the y axis is reported the number of experiments.

To better represent the phenomenon, the logarithm of soot was used as output and new Neural Networks were then trained with the 3 input patterns described.

The application of the logarithm has two effects on the model: the first one is a more homogeneous distribution of all the points on the interval; the second one is a reduction of the error percentage. The correlation coefficient also increases, as it is possible to observe in the Table 4-8.

In Figure 4-33 it is possible to observe a more homogeneous distribution of the outputs of the Neural Network and an increase in the correlation coefficient both on the Test Set, from about 0.85 (Figure 4-31 left side) to about 0.95 (Figure 4-33 left side), and across the entire Dataset from about 0.97 (Figure 4-31 right side) to about 0.98 (Figure 4-33 right side).

Similarly, the percentage errors between measured data and Neural Network output also vary from a range of about -200% to about 500% (Figure 4-32), for the Neural Network trained with soot outputs, to an error range of about -50% to 50% (Figure 4-34) for the Neural Network trained with log(soot) outputs.

From these considerations it follows that to have a more accurate simulation of soot is necessary a change of the scales from linear to logarithmic. For the application of this model it is worth to set to zero the few negative values computed by the Neural Network. Moreover, for real field

implementation, further investigation on the neural network transfer functions with always positive output should be done.

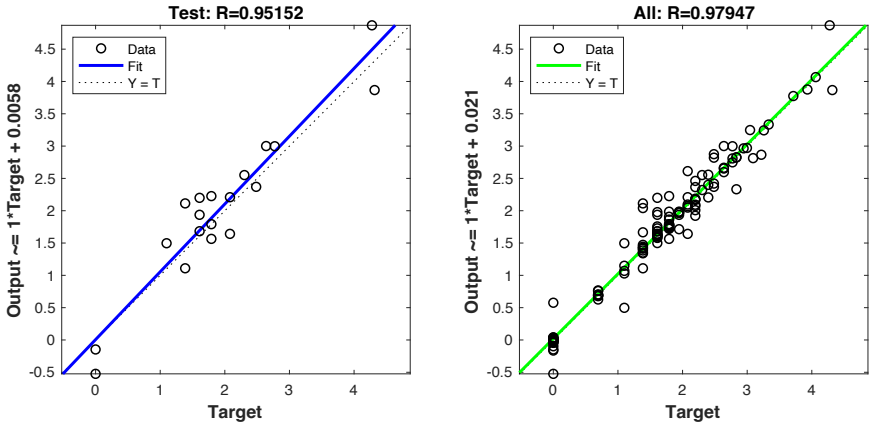

Figure 4-33 On the left, the measured vs calculated data on Test Set; on the right, the measured vs calculated data on all the experimental points. The network considers the logarithm of soot. The Network has 13 neurons in the Hidden Layer and the input pattern is the #2 (see Figure 4-29).

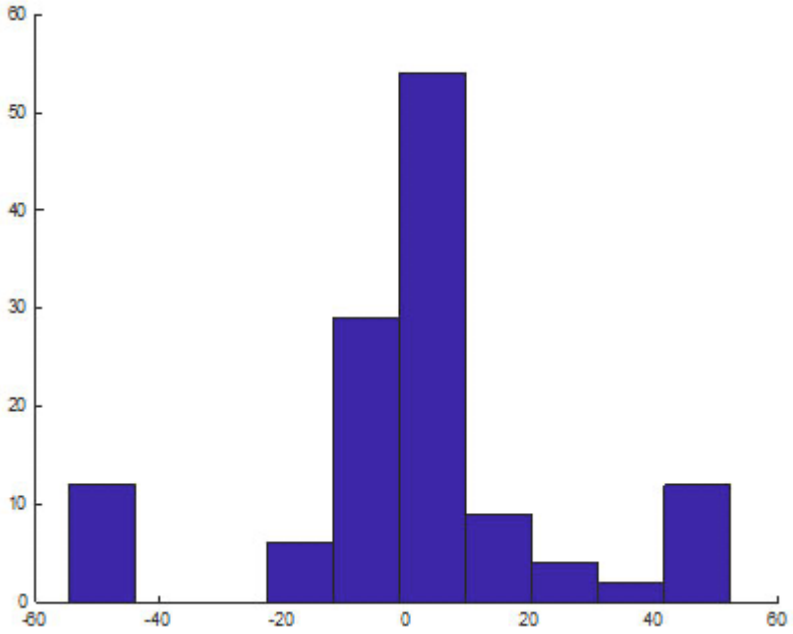

Figure 4-34 Distribution of error percentage for the logarithm of soot. Neural Network with 13 neurons in the Hidden Layer and input pattern #2 (Figure 4-29).

Table 4-8 Comparison of correlation coefficients of network output.

	SOOT	log(SOOT)
Number neurons of Hidden Layer	13	13
Epoch	26	45
Best epoch	20	39
Max R^2	0,9417	0,9594
Mean R^2	0,5555	0,8455
Min R^2	0,0002	0,3988
Relative variation	0,9416	0,5606
Percentage relative variation	99,98	58,43
Mode	0,5204	0,8776
Median	0,5565	0,8527
Variance	0,0202	0,0042

CHAPTER 5
Technologies for information-driven Control Systems

In this chapter is discussed the application of Artificial Neural Networks for calculating the efficiency and emissions of a micro-cogeneration system consisting of a boiler with a Stirling engine described in chapter 3.

These networks are part of an integrated IT system for the remote management of the cogenerator, The IT system is described in the first paragraphs of this chapter.

5.1 An intelligent plant system for hot water heating.

This section describes an installation of an intelligent computer system for hot water heating. In particular, for the proposed solution, the energy production phase is based on a boiler operating in electrothermal cogeneration mode. For the development of the integrated computer system, a fundamental part is covered by the application of Artificial Neural Networks. These Networks were obtained by resorting to a preliminary methodology based on linear regression for the reduction of the parameter space.

The objective of the entire IT system is to manage and optimize the following aspects for the monitoring and control of the cogeneration system:

- Anomalies and maintenance interventions;
- Energy consumption;
- Fluids;
- Fumes.

The aim is to investigate the thermal response deriving from various load profiles (both thermal and electrical) in order to generalize their use for a wide range of Stirling engine boilers.

The entire IT system will be installed in a control unit for detecting/controlling the operating parameters of the cogeneration system (indicated by the "Control Unit" component in Figure 5-1).The Control Unit will be in communication with the central server and will provide the optimal operating parameters for the different operating contexts of the cogeneration systems. The specialized models developed here, trained and validated on theoretical data, will be used to analyze the real boiler operating data, in combination with meteorological data (OpenWeatherMap).

The proposed model has been formulated for the datasets available in the literature and is inspired by the models and techniques applicable to the problem of representing, analyzing and correlating data from boilers.

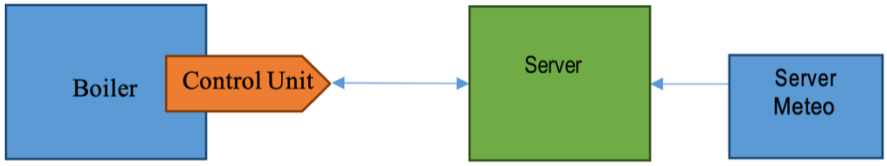

Figure 5-1 Integrated informative system on a boiler.

5.1.1 The Boiler

The boiler is the heart of the plant, where the fuel is burned to heat the water or air (heat transfer fluid) that will then circulate in the user plant, and to produce electricity, thanks to the cogeneration subsystem. In general, it consists of a burner that mixes the air with the fuel and feeds a combustion chamber (the *hearth*), a series of tubes through which the hot fumes produced by the combustion the heat carrier fluid and an external casing made of an insulating material protected by a thin metallic wall (insulating shell).

In this cogeneration system, the heat from the boiler is used to generate electricity by means of the Stirling machine (see chapter 2). This additional, allows to further optimize the boiler efficiency thanks to proper control actions.

The term Stirling machine (Naso, 1991) (Redlich & Berchowitz, 1985), refers to a wide range of fluid machines, in which the fluid itself carries out a thermodynamic cycle close to the ideal Stirling one (consisting of two isothermal and two isochore transformations, as shown in section 2.3). The

motion of the fluid is not regulated by valves or other equivalent devices, but by the variation of the working volumes occupied by the fluid inside the machine itself.

5.1.1.1 Power Delivered

With respect to the project objectives, each boiler is characterized (but also represented) by:

- the thermal power output of the fireplace, which indicates the amount of energy that the fuel develops in the combustion chamber in an hour;
- the useful thermal power, that is, the energy actually transferred, for each hour, to the heat transfer fluid;
- the electrical power generated by the cogenerator.

The management optimization offers a large gain in terms of both savings and emissions and improves the performance of the cogenerator which is greatly influenced by the different operating profiles of the system. In fact, the heat produced by the fuel is partly transferred to the thermo-vector fluid, but a fraction is dispersed towards the outside by the body of the boiler itself (through the insulating shell) and above all by the fumes that come out, still hot, from the chimney.

In this process, the cogeneration of electricity recovers part of the dispersed thermal energy and improves the efficiency of the system. In fact, the closer the power values to the firebox are to those of the useful power, the lower the heat losses and therefore the better the boiler efficiency. Table 5-1 (CNAE Energia, 2015) shows, by way of example for each type of boiler, some values for the minimum efficiencies that can be used as a comparison to evaluate performance.

Table 5-1 Differences between the Useful Power and Efficiency for different types of Boiler.

Type of Boiler	**Useful Power**		**Efficiency at nominal Power**	**Efficiency at partial load**
	KW	**Kcal/h**	**%**	**%**
Standard Boiler	20	17200	86,6	83,9
	200	172000	88,6	86,9
Standard Boiler with high efficiency	20	17200	89,5	89,5
	200	172000	91,0	91,0
Condensing Boiler	20	17200	92,3	98,3
	200	172000	93,3	99,3

The choice of power and type of boiler to be installed depends on the characteristics of the building, its location and its intended use. The sizing of the boiler affects the performance of the entire system.

In fact, a larger than necessary standard boiler wastes energy: especially in autumn and spring, it quickly reaches the preset temperature and therefore has long and frequent shutdown periods during which it disperses the heat from the mantle and through the chimney. In particular, in case of the entire heating season, its overall efficiency is not high, that is, its seasonal performance is low. In order to comply with the efficiency values imposed by the new standards, the most recent boilers such as "modulating", "sliding temperature" and condensing boilers allow to maintain good efficiency even in intermediate seasons.

5.1.2 Thermostatic Valves

In both centralized and single (i.e., one heating per apartment) systems, great strides have been made in the direction of consuming energy only where and when it is needed. Also, with a view to a future integration with the Internet of Things, every single heating point can be an “intelligent object”. With the addition of a thermostatic control with remote control/reading, the temperature of each individual room can be adjusted to take advantage of the free energy inputs, i.e. those due, for example, to the presence of many people, to the sun's rays through windows or appliances in operation. It is already a widespread practice to equip each radiator with a thermostatic valve to automatically adjust the inflow of hot water based on the temperature chosen on a graduated knob. The valve closes progressively as the room temperature approaches that set by the thermostat, allowing further hot water to be diverted to the other radiators, which are still open. In this way, less energy can be consumed on more hot days, when the sun is sufficient to heat some rooms, or, for example, set a lower temperature in the bedrooms and a higher temperature in the bathroom or even leave the radiators open to the minimum when nobody is in the house. The thermostatic valves installed in centralized systems also have a good influence on the thermal balance of the different areas of the building. When the hottest floors reach 20°C, the valves close the radiators allowing a greater inflow of hot water to the cold floors.

The energy savings induced by the use of thermostatic valves can reach up to 40%. Precisely for this reason, installation in new buildings and renovations is often mandatory (TATANO s.n.c., 2020).

5.1.3 Condensing Boilers

The higher efficiency values typical of condensing boilers depends on the ability to condense the water vapor in the burned gases (i.e., the fumes) discharged outside. Since the cooling of the fumes is operated by the water returning from the heating system, the lower its temperature, the greater the cooling capacity and the amount of heat recovered from the fumes by the condensing boiler. According to these considerations, in new buildings it is recommended to combine condensing boilers with low temperature heating systems, such as underfloor or radiant wall systems. Moreover, radiators with large surface improve the heat exchange with the rooms to be heated, thus lowering the temperature of the returning water, which in turn guarantee a better heat recovery from the condensing of water in burned gases. If, on the other hand, a standard boiler needs to be replaced with a condensing one and the existing heating system does not fall within the types listed above (i.e., there is a traditional type system designed to work at average water temperatures of 70° C), the energy saving potential offered by the condensing boiler will be limited.

When the external temperature will drop below -5 ° C (design temperature on which the heating system is configured) the return water temperature will be too high to allow condensation and therefore the condensing boiler will behave like a traditional boiler. In the remaining periods in which the heating system is active and the external temperature is higher than the design one, the control units with probes detects the external temperature and the system produces water at lower temperatures, which allow the condensation of steam and the energy recovery.

In summary, to optimize the average seasonal efficiency of a condensing boiler it is necessary to:

- minimize the water return temperature in the boiler through the proper choice of the heating elements used;
- maximize the periods in which the boiler works at low power in order to minimize the final temperature difference between fumes and water, by reducing intermittent operation;
- always maintain a stable and limited excess of air, by coupling a premix burner with an optimal adjustment of the fuel/air mixture.

The choice of materials for the pipes to be coupled to the condensing boilers must take into account the presence of condensate and the possible corrosive effect at the temperature of the fumes. It is therefore necessary to use corrosion-resistant materials, such as stainless steel, but, thanks to the low temperature of the discharged fumes, it is also possible to use plastic pipes.

Condensing boilers also require the presence of a pipe for the discharge of condensate water.

5.2 Data Analysis and Control Techniques

The mathematical model proposed in the following Sections has been obtained adopting Artificial Neural Network concepts previously introduced and Numerical regression.

5.2.1 Numerical Regression

In general, regression is used to explain the relationship between a (continuous) variable Y called response variable (output or dependent variable), and one or more variables called covariates, explanatory, independent variables, or regressors, predictors or input variables. $(x_1, x_2, \dots, x_k)$. In functional terms:

$$Y = f(x_1, x_2, \dots, x_k) + \epsilon \quad (5.1)$$

which indicates the existence of a functional link, on average, between the dependent variable and the regressors, represented by the component $f(x_1, x_2, \dots, x_n)$ and which is usually given the name of systematic component. To this exact functional component, another one, called accidental, random, erroneous, is added.

While the first represents the part of the response variable explained by the predictors, the second component represents that part of the variability of the response that cannot be traced back to systematic or easily identifiable factors, but due to chance and, more generally, to different causes not taken into account in the regressive model.

In theory, the functional link can be of any type, but in practice it is preferable to use a linear function and therefore the multiple linear regression or linear model is used, which assumes the following formulation:

$$Y = \beta_0 + \beta_1 x_1 + \ \dots + \beta_k x_k + \epsilon \quad (5.2)$$

where ϵ is called the known term, while $\beta_1, \dots, \beta_k$ are called regression coefficients and, together with the variance of the error, are the parameters of the model to be estimated on the basis of sample observations.

Different models, apparently non-linear, can be linearized through suitable transformations of variables.

For example, the multiplicative model:

$$Y = \beta_0 x_1^{\beta_1} \ldots x_k^{\beta_k} \epsilon \quad (5.3)$$

can be easily transformed into the linear model by applying logarithmic operators to both sides.

It is called polynomial regression when the regressors of the model are involved in the regression formula not only with degree equal to one, but also with greater degrees.

In the prototype proposed, regression will be introduced as a technique to be applied to the boiler operating parameter space to reduce its size and consequently shorten the training time of the Neural Network. Pending the availability of real data, which will be provided by the system control units once fully operational, the most influential operating parameters with respect to the objective to be optimized are established by choosing, from scientific works on the subject, likely factors to be used for training of the system and obtain the commands to send to the boiler, due to the change in the operating data. In this perspective, the regression does not find a justification at the level of this neural prototype and will be carried out only before training on the fully operational data. (Spriet & Vansteenkiste, 1988) (Montgomery, 2013)

5.3 Numerical model

For the development of the neural model two methodological steps have been conceived, which will be exploited upon the implementation of the system's control unit and its application on field.

The first step uses a regression model for the interpretation of the operating data of the boiler to identify the independent variables, based on the influence on the performance. Afterward, that model selects the data relevant to the most significant regressors associated to the boiler consumption and efficiency performance data (i.e., the dependent variables); then the training samples of the neural system are used as input for the Neural Network (second step). Such an approach allows reducing the parameter space, thus limiting the computational complexity of the training algorithms. Due to the lack of real data, the first step has not been implemented to decide the most influential operating parameters with respect to the variables to be optimized.

For the purpose of this work, the proposed model has been developed and validated using the data available from the literature for the purpose of training the neural controller.

Appropriate synthetic data were chosen starting from the Gas Boiler Test Results - Morrin UCD Dataset (Morrin, 2015), from those made available by USEPA (USEPA, 2015) and from the measurements offered by the Politecnico di Milano (LEAP, 2015) as well as by the "Ordine degli Ingegneri" of Cagliari (Ordine degli Ingegneri di Cagliari , 2015).

The answer to the problem of optimal management of the heating system can be provided by calculation tools that allow to optimize the combustion set-up reducing both the emissions of the main pollutants and the specific fuel consumption (CESI, 2015) of the cogeneration system. These tools use artificial intelligence techniques to develop a model that relates the controllable quantities with the emissions and the efficiency of the process. The advantage of adopting models based on Neural Networks lies in the possibility of building a model following an inductive process, guided only by the processing of experimental data acquired on the plant. This avoids the development of models based on the physical laws of several complex processes whose an accurate mathematical synthesis (i.e., the model) could be awkward to be accomplished.

The objective of computing the optimal control variable is achieved by coupling the predictive Neural Network model with an optimization algorithm. As sketched in the scheme of the Figure 5-2, the Optimization Algorithm computes the control variables (i.e., the vector *u* in the **Figure 5-2**) that optimizes the system performance minimizing both emissions and specific fuel consumption. In the process some constraints (load determined by temperature difference and electrical energy demand of cogenerator) are imposed by the control system.

On the real system, the control stgructure thus obtained will be automatically implemented by the boiler control units (Figure 5-2).

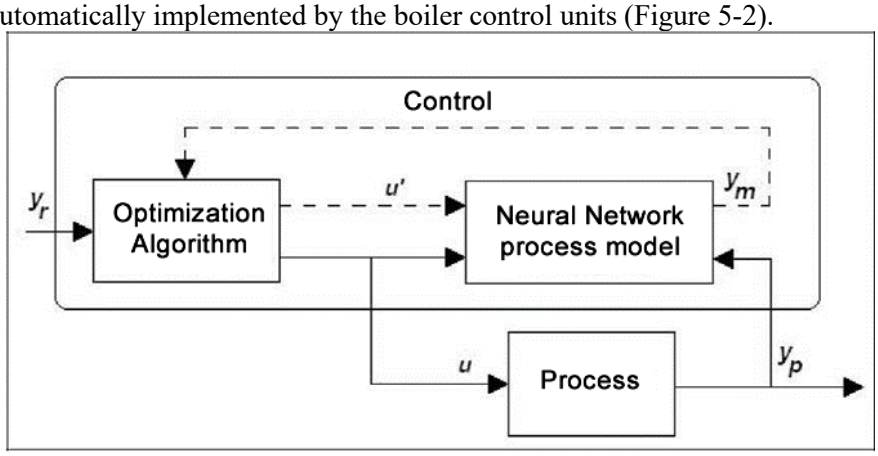

Figure 5-2 Configuration Control Unit: *u* real operative condition; *u'* operative condition calculated by Optimization Algorithm; y_m output of Neural Network model; y_r costraints; y_p objective variable obtained as output of the real process.

The problem of optimization of combustion in boilers is set as a problem of minimization of specific consumption, guaranteeing a reduction of CO_2 emissions. It is worth recalling that the minimization of polluting emissions is more critical because performance (e.g., fuel consumption) and emissions, could be often antithetical. Therefore, the a set of weighting factors should be considered while building the objective function to be minimized, thus giving more emphasys on either performance improvement or polluting emissions reduction.

For certain operating variables (e.g., u'), the model calculates the expected values of the quantities y_m to be optimized, which may also be constrained and kept below a threshold. These y_m variables are returned to the non-linear optimization algorithm which decides the variations to be assigned to the operating values indicated in the next step and returns them as input to the model.

The process is repeated until y_m values are obtained which minimize the objective function in compliance with the y_r constraints. At this point, the operating values can be set on the system and produce values of the target quantities y_p, which are in turn also used to update the Neural Network model.

The implementation of this technology allows to establish the operating values that must be set by the control system according to the actual conditions of the cogenerator and the rest of the plant and, therefore, with less conservative and generally more advantageous values, but requires the availability of real data on which to train the neural system.

From data available in the literature, it is assumed that the expected benefits from the application of such an online control system are around 0.3 ÷ 1.0% reduction in specific consumption and 10 ÷ 15% reduction in polluting emissions, with a return on investment within the first year of use. (Pretolani, 2003) (Pretolani & Tassi, 2000a) (Pretolani & Tassi, 2000b) (Sarunac, et al., 2003)

Figure 5-3 outlines the environmental, setting and operating parameters that are used as input/output between the control unit and the boiler in the prototyped model in this work.

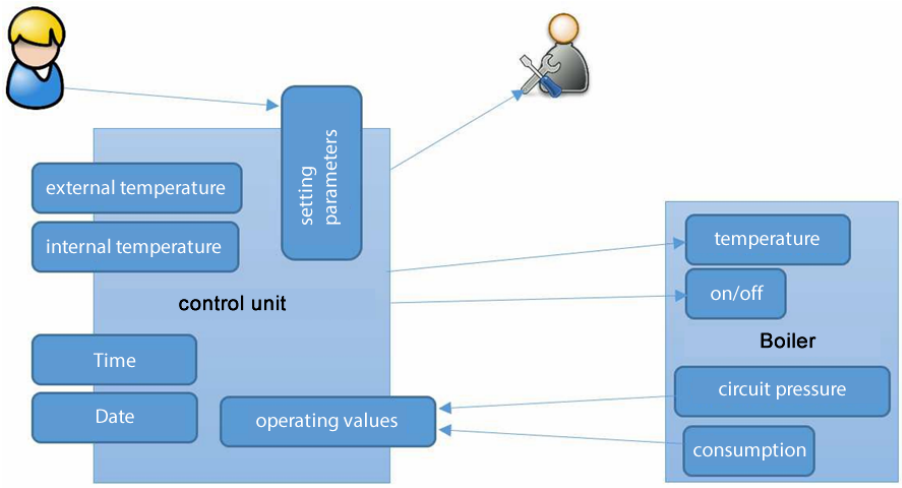

Figure 5-3 The parameters of boiler and control unit.

According to the Figure, the overall control unit can switch on and off the boiler and adjust its main parameters. The control unit sends the appropriate commands to the boiler according to the external and internal (i.e., apartment) temperature with a seasonal strategy. Moreover, the control unit also receives the operating values (consumption, internal temperature of the house and pressure of the heating circuit) and can decide to request maintenance if it detects abnormal behavior in the boiler.

5.3.1 The Neural Model

The control unit prototype for this work proposes the adoption of Neural Networks used as simulators of mathematical functions and in particular as a simulator of the behavior of the boiler and the heating system. On the basis of the training Dataset, the network is able to understand the function that links output with input. Moreover, thanks to the generalization capabilities of the neural system adopted the trained network is able to provide an output also in response to input other than those used as training examples. This capacity is useful in the case of the control unit for managing the heating system even if the link between input and output does not have an explicit mathematical structure. The network behaves like a "black box" and does not require the formalization of the transfer function that is contained within it. Nowadays, the adoption of Neural Networks allows easy physical implementation of the control unit thanks to the availability of processors that integrate circuits

dedicated to their execution. Therefore, the proposed algorithm could be straightforward applied on commercial systems.

Two of the neural models adopted as a prototype for this work are the Neural Networks represented in the Figure 5-4 and Figure 5-5, they differ in architecture and classification/computation capacity. Eventually, these networks will be replaced by a simpler neural infrastructure that guarantees the same accuracy with faster learning. Obviously, the synthetic data used for the experimentation and the architecture of the subsystem will have to be readjusted, once new real data will be available.

Both networks are designed to receive four inputs that represent the "polluting" state of the control unit-boiler system:

- CO_2 emission;
- CO emission;
- NO_X emission;
- Combustion efficiency.

The first Network (Figure 5-4) has a structure with a single Hidden Layer composed of 8 neurons, completely connected between input and output.

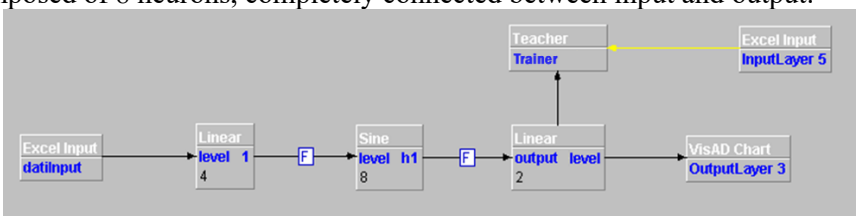

Figure 5-4 Neural Network with a single Hidden Layer

The second Neural structure (Figure 5-5) proposed is more complex with respect to the previous one, indeed the architecture is changed by adding an additional Hidden Layer, composed of 8 neurons and completely connected to the rest of the system (**Figure 5-2**).

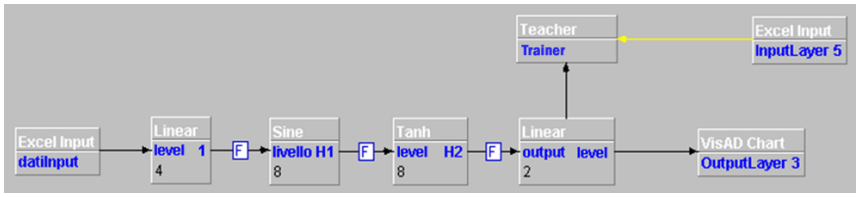

Figure 5-5 Neural Network with two Hidden Layers.

The two outputs of both networks provide the injection of gas and power values that the neural subsystem suggests in order to minimize the emission of the heating system by maximizing its yield.

5.3.2 The Training Dataset

When the system is up and running, the data for monitoring the parameters controlled by the boiler control unit are transmitted to the center with a sending frequency that can be accommodated at the request of the control center. For example, in case of anomalies, other information can be added with respect to ordinary parameters, which are, typically, consumption and emissions.

Below is the list of parameters grouped by category:

1. Measurements of fumes:
   - CO_2 emission;
   - CO emission;
   - NO_X emission;
   - Combustion temperature;
   - Combustion efficiency.

2. Measurements of fluids:
   - Inlet water temperature;
   - Temperature of the water at the outlet;
   - Water flow.

3. Energy measurements
   - Electric power;
   - Thermal power.

The data to train the system is not yet available, but, as shown in the next section, the neural subsystem can be considered a "black box", independent from the rest of the subsystems belonging to the ecosystem. This will allow to improve the behavior of the control unit without impacting on the other subsystems that use it.

5.3.2.1 Emissions

In Figure 5-6, Table 5-2, Table 5-3 is represented the synthetic Dataset used for the training of the neural subsystem. It was obtained starting from the detection of the pollutants of interest, consisting of CO, NO_x and total VOC (disaggregated into methane and non-methane-NMVOC), measured by two multiparameter analyzers.

In particular, reference was made to the data of the E.C.A.T.E. project, Efficiency and Environmental Compatibility of Energy Technologies (LEAP,

2015)]. From the paper, it is also possible to derive the main combustion parameters (temperature, CO_2 and oxygen content of the fumes), as well as the environmental and energy parameters required for a correct quantification of the emission regime of the appliances in the different operating conditions.

The observations used to create the Dataset were performed both at low load (30% of available power) and at full load (100%).

Table 5-2, Table 5-3 show the data concerning the emissions of pollutants that were taken from the report of the E.C.A.T.E. project.

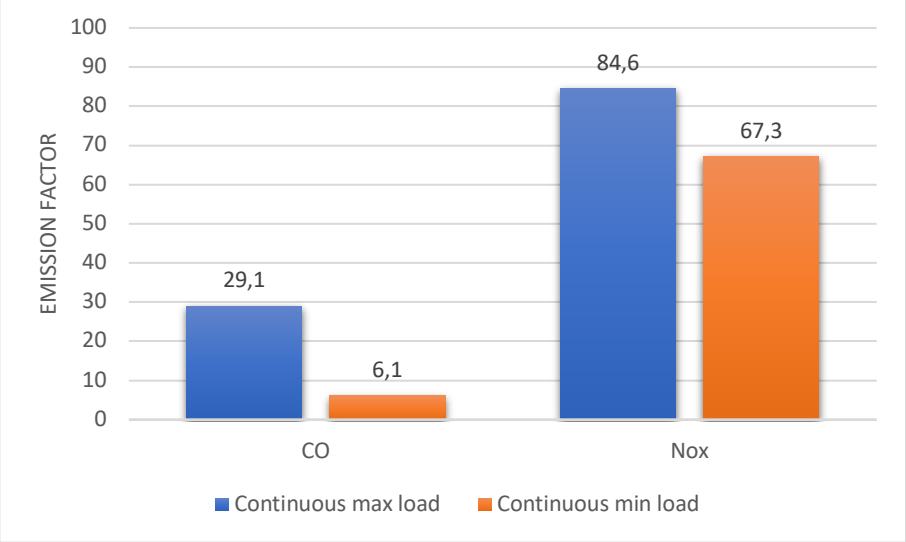

Figure 5-6 Emission factor of CO and NO_x at maximum and minimum load.

Table 5-2 Emission data at minimum and maximum load (1/2).

Operating Regime	O_2 m(%vol)	Concentrations (mg/Nm^3 3%O_2)		Emission factors (g/GJ)	
		CO	NO_x (*)	CO	NO_x (*)
Continuous max load	7 (6,7-7,6)	85,3 (79-89)	247 (226-272)	29,1 (27-30,4)	84,6 (77,4-93,2)
Continuous min load	14,1 (13,1-15)	20,3 (11-35)	196,5 (103 -313)	6,9 (3,8-12)	67,3 (35,3-107,2)

Table 5-3 Emission data at minimum and maximum load (2/2).

Operating Regime	O_2	Concentrations			Emission factors (*)		
	(%vol)	(mg/Nm^3 3%O_2)			(g/GJ)		
		VOC (**)	Methane	NMVOC (***)	CO (**)	Methane	NMVOC (***)
Continuous max load	7	1,5	0,4	1,1	0,4	0,1	(n.r.-0,5)
	(6,7-7,6)	(0,3-3,5)	(0,3-1,7)	(n.r.-1,8)	(0,08-0,9)	(0,08-0,4)	
Continuous min load	14,1	7,2	5,9	1,3	2,1	1,7	0,4
	(13,1-15)	(5,7- 10,8)	(4,7-7,1)	(1- 3,7)	(1,7-3,1)	(1,4-2)	(0,3-1,1)

The model presented in this report has been formulated considering CO emissions and efficiency of cogeneration systems. The fully operational data, similar to the synthetic ones shown in this document, will allow the training and validation of specific Neural Networks for the modeling of each factor detected by the control unit.

A first analysis on the data used for the modeling of the Dataset shows CO emissions at the maximum thermal load placed around 30 g/GJ, corresponding to concentrations in the range between 80 and 90 mg / Nm^3 at 3% of O_2, with NO_x present at higher levels, equal to about 85 g/GJ (concentrations between 220 and 270 mg / Nm^3 at 3% of O_2). In line with the decrease in fuel consumption, the corresponding values measured at minimum load appear lowered: notably, reductions are observed for CO, with average emissions of 7 g / GJ and concentrations between 10 and 35 mg / Nm^3 at 3% of O_2, while NOx shows less consistent variations, with decreases up to about 70 g / GJ and mean concentrations around 200 mg / Nm^3 at 3% of O_2. The results of the measurements at minimum load also indicate greater fluctuations in the measured concentrations, with wider ranges of variation which seem to indicate a certain difficulty in maintaining combustion stability in the most extreme operating conditions compared to the nominal ones. Adjustment difficulties in this regard are also observable from the considerable excess of air maintained at minimum load, with an increase in the oxygen content of the fumes from about 7% – detected in nominal conditions – up to 14%. Compared to CO and NO_x, total hydrocarbon emissions (VOC) exhibit an opposite behavior, with the levels measured at nominal load, equal to 0.4 g / GJ, which undergo an appreciable increase at minimum load, reaching approximately 2 g / GJ. On the other hand, the status observed at nominal load, the splitting into methane and non-methane hydrocarbons (NMVOC) shows a large prevalence of unburned methane in operating conditions at reduced load; thus confirming the difficulties already mentioned above in obtaining a stable combustion during operation at minimum power.

In particular, for the preliminary validations of the model proposed, the values of CO emission were considered, and the reported measurements were interpolated to extend the data to the entire range of emission values relating to different load regimes of the boiler. The lack of field data, which will also allow the correlation between emissions and actual boiler efficiency, the neural system has been trained with the data presented before, which were

interpolated over the whole interval. Therefore, CO emissions were interpolated, on the entire scale of the boiler load regimes (0-100%) and the values obtained were used for training the neural system.

Figure 5-7 shows the CO emission curve obtained by interpolating with a cubic spline the information from the E.C.A.T.E. project report, in the graph 100 uniform samples between 0 and 100 were considered (see red curve).

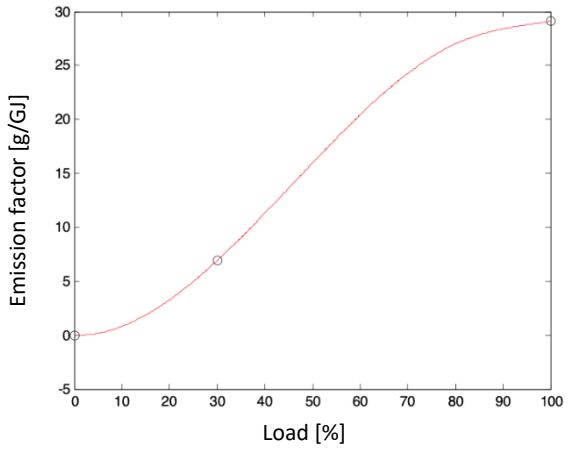

Figure 5-7 Curve of CO emissions obtained through spline interpolation.

To simulate the variability of the systems connected to the control unit, a uniform random noise signal in the interval [-5.25, 5.25] was added to the previous interpolation data in order to understand the robustness of the developed prototype with respect to noise on the measurement signals.

Figure 5-8 shows the disrupted trends in CO emissions.

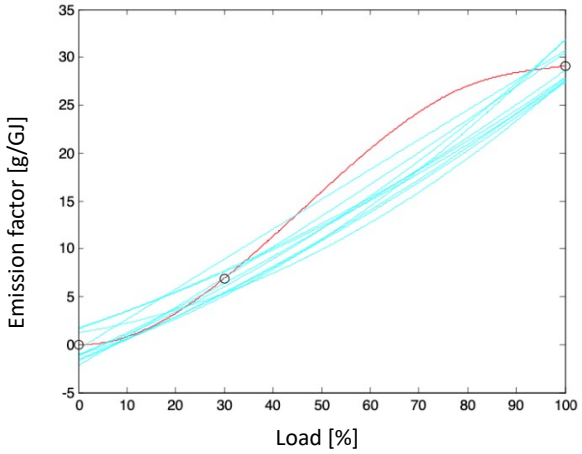

Figure 5-8 Robustness verification of the proposed model (red curve) with random perturbation of the data obtained (cyan curves).

In Figure 5-9 it is shown the same uniform random noise allowed a subsequent verification of the robustness of the proposed model by superimposing two other sources of uniform noise on the sampling Dataset in the interval [0.5, 5] (black curves) and in the symmetrical [-5, 5.0] (blue curves).

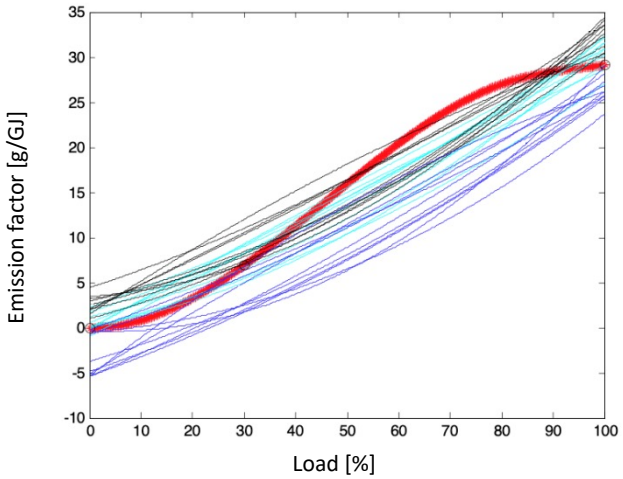

Figure 5-9 Robustness check of the proposed model (red curve) with further random perturbations of the Dataset.

5.3.2.2 Performance

The information to model the performance was extracted from the Cost/Benefits analysis in (Cutler, et al., 2014), which shows the efficiency values of the condensation boilers with respect to the percentage of power supplied (load factor) and the external temperature.

The Figure 5-10 shows the curve that was used to model the boiler efficiency and prepare the neural subsystem training Dataset (see the yellow curve).

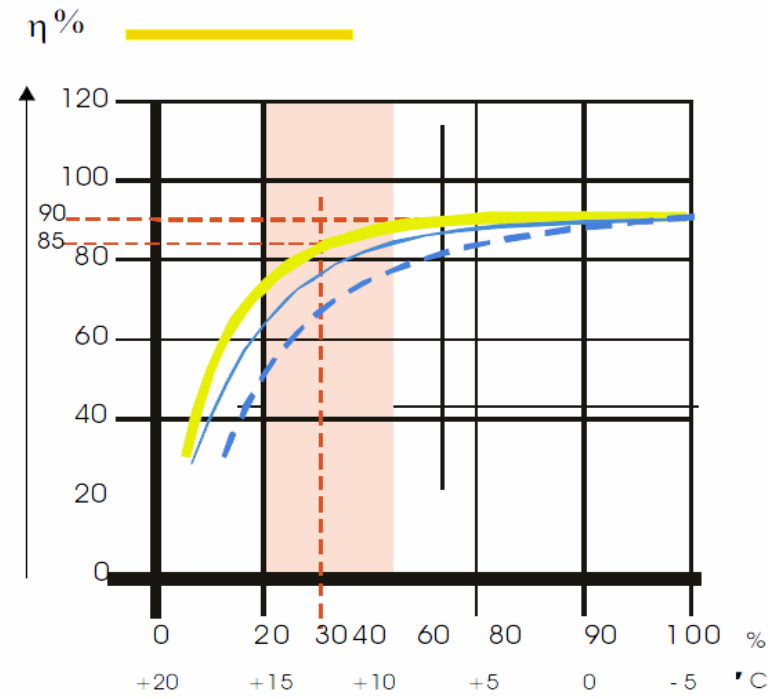

Figure 5-10 Efficiency curve (in yellow) as a function of the loads and temperatures of the external environment.

It is worth noting that the efficiency values corresponding to the load factors were measured starting from 10% (η = 51%) up to 100% (η = 90%). These data, associated with the emission levels, were used for the training of the neural system.

Table **5-4** shows the sampled performance values that have been interpolated with cubic spline (100 uniform samples between 0-100, shown in Figure 5-11).

Table 5-4 Load and efficiency Dataset.

Load Factor	10%	20%	30%	40%	50%	60%	70%	80%	90%	100%
Efficiency (η)	51%	70%	82%	86%	87%	88%	88%	89%	89%	90%

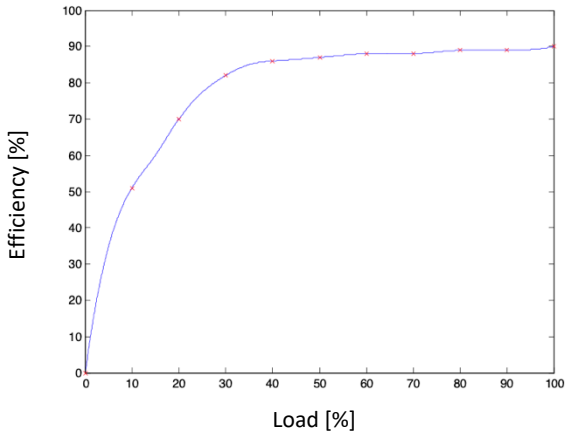

Figure 5-11 Interpolation of the Dataset with a spline curve.

To simulate the variability of the systems connected to the control units, a uniform random noise in the interval [-10.25, 10.25] was also added to the previous interpolation data in order to also understand the robustness of the developed prototype with respect to the noises on measurement signals (Figure 5-12).

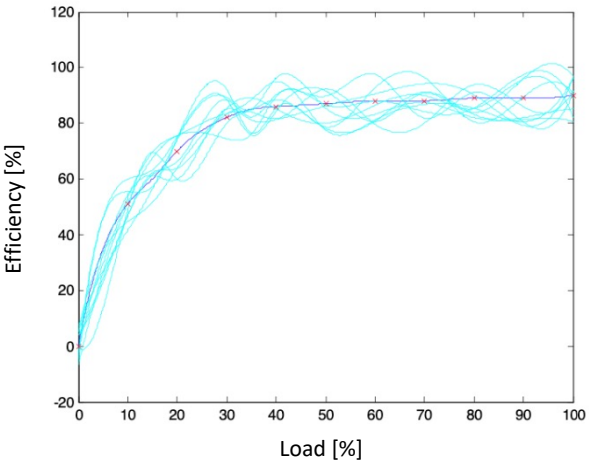

Figure 5-12 Verification of robustness of the efficiency model with the introduction of a random noise source.

A further verification of the robustness of the proposed model was performed by adding to the sample Dataset two other sources of uniform noise in the interval [0, 20.25] (black curves in Figure 5-13) and in the symmetric [-25.5, 0] (blue curves in Figure 5-13).

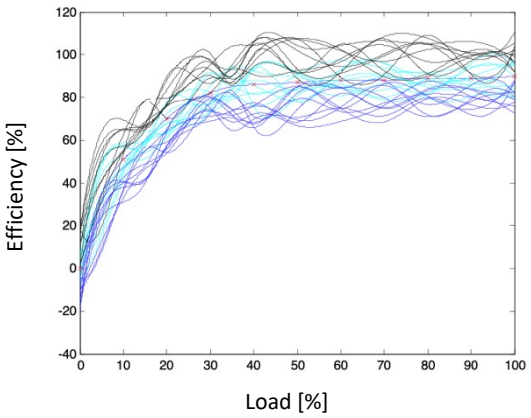

Figure 5-13 Verification of robustness of the performance model with the introduction of multiple random noise sources.

5.4 Validation

The neural architectures proposed previously have been simplified and reduced to a Neural Network with 10 hidden nodes, which represents the right compromise between training complexity and predictivity capacity

As it will be shown in the description of the Neural Network training, this setup achieves optimum performance, but it should be noted that it may vary with actual data from boilers.

In addition, the data preprocessing phase, based on the application of regression techniques to choose the operating parameters of the boiler that are most correlated to the optimization of its performance, will be carried out only on the system in operation, when the data will be available, real info recorded by the control units.

Recalling that the neural subsystem will be used to model the heating system and its response to the control unit commands, the validation on synthetic data proposed in this report starts with training on the data obtained from the literature and relating to the production of CO and efficiency of the cogeneration system. Once the neural control has been trained, its goodness of representation will be validated by measuring the simulation error in the case of a sample excluded from the Training Set. Although training is not a deterministic process, it always introduces characteristics of variability. The Appendix reports both the training and validation samples for the datasets used (i.e., CO emissions and system performance).

5.4.1 CO emission model

The synthetic Dataset used for the training of the neural subsystem was obtained starting from the detection of the pollutants of interest, consisting of CO, NO_x and total VOC (disaggregated into methane and non-methane-NMVOC), measured by two multiparameter analyzers. In particular, reference was made to the data of the E.C.A.T.E. project, and to the document EMISSION CHARACTERISTICS OF INDEPENDENT HEATING UTILITIES CIVIL (Cernuschi & Consonni, 2016).

The Neural Network was trained with 100 spline interpolations of the measures best described in Section 5.3.2. The CO emissions inferred from the document were interpolated across the full scale of load factors (0% -100%) and the values obtained were used for training in the simulation of CO emissions (Figure 5-14).

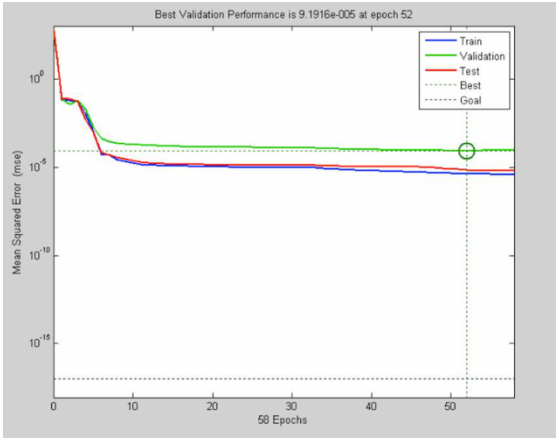

Figure 5-14 Neural Network training results for CO.

The first observation made during the training of the Neural Network was on the rapid convergence of the system which reaches a capacity significantly representative (with a mean square error of the order of 10^{-4}) already after less than 10 epochs (training cycles), as shown in the Figure 5-14 by the green curve.

To validate the proposed approach with respect to the CO emission model, the output of the network was compared with the expected values from operating configurations not used for training.

The next graph is the synthetic curve of CO emissions obtained by interpolating the information obtained from the E.C.A.T.E. project report with a cubic spline. The values have been interpolated with a cubic spline from which 100 uniform samples in the range of operating regimes [0-100] have been extracted. Similarly, in points other than the first 100, the 10 points used for the validation of the neural system were sampled.

As shown Figure 5-15 the behavior of the spline that interpolates the original measurements (red curve) and that of the Neural Network performed on the validation sample (blue curve), are in fact indistinguishable (unless there are differences in density in the sampling). In fact, the measures are detached by a maximum error of the order of a tenth of g / GJ (the errors of representation are shown in Figure 5-16).

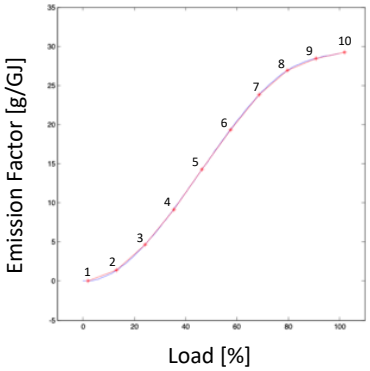

Figure 5-15 CO Dataset trend (red curve) vs Neural Network results (blue curve).

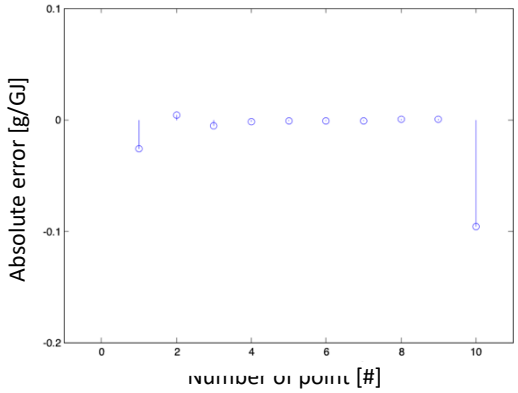

Figure 5-16 Absolute error between CO calculated by the Neural Network and the Dataset.

5.4.2 Efficiency Model

The information to model efficiency was extracted from "Condensing boilers Evaluation: Retrofit and new Construction Applications" (Cutler, et al., 2014), which reports the efficiency values of condensing boilers with respect to the percentage of power supplied (load factor) and the external temperature.

In particular, the efficiency values corresponding to the load factors were measured starting from 10% (η = 51%) up to 100% (η = 90%). These values, associated with the emission levels, were also used for the training of the Neural Network.

The efficiency values were interpolated with a cubic spline from which 100 uniform samples between 0-100 were extracted. Similarly, in points other than the first 100, the 10 points used for the validation of the neural system were sampled.

Also in this case, the first observation is on the rapid convergence of the system which, already after 5 training cycles, reaches a remarkable representative capacity, as shown in Figure 5-17 by the green curve.

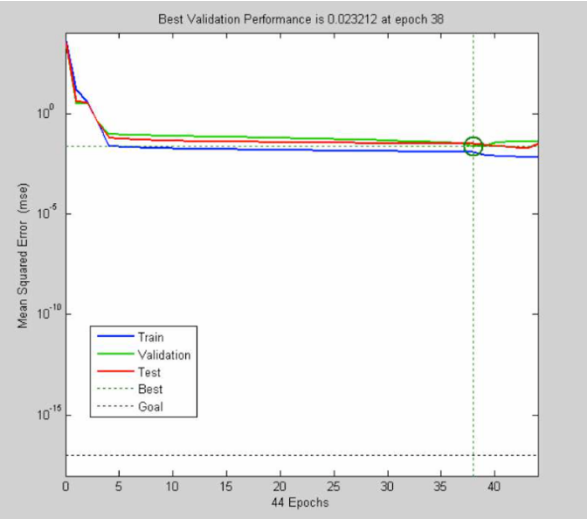

Figure 5-17 Neural Network training results for Efficiency.

As shown in Figure 5-18, at the end of the training, the behavior of the spline that interpolates the first measurements and that of the Neural Network performed on the validation sample, are in fact indistinguishable with a maximum error of the order of the tenth of the unit yield factor (the representation errors are shown in Figure 5-19).

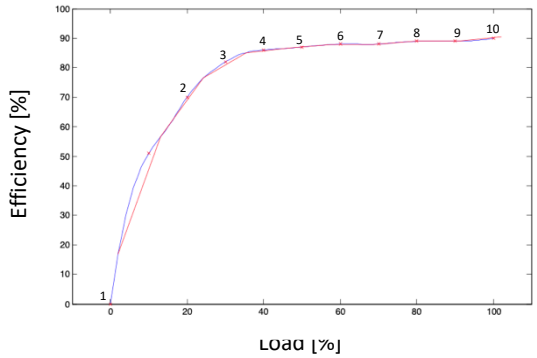

Figure 5-18 Efficiency Dataset trend (red curve) vs Neural Network results (blue curve).

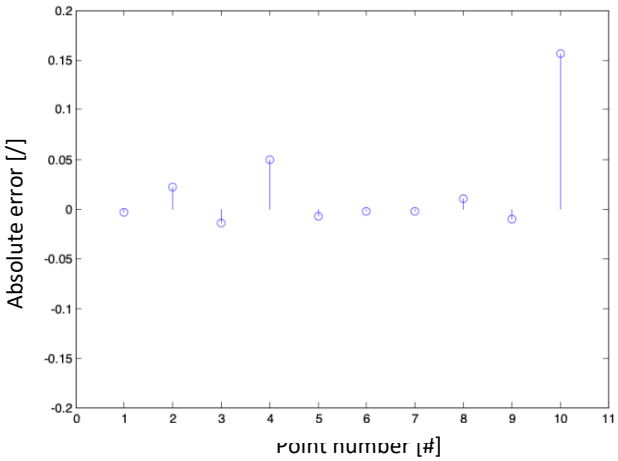

Figure 5-19 Absolute error between Efficiency calculated by the Neural Network and the Dataset.

5.5 Final Remarks

It is worth mentioning that the aim of the work is to create an algorithm to be inserted into an integrated monitoring and control system for the management of domestic micro-cogeneration systems. As described in chapter 2, there are numerous types of domestic micro-CHP, which differ both structurally (pairing with an electric generator) and in the type of fuel used (methane, LPG, pellets, ...), it would have been difficult to formulate exact and explicit models of these devices in order to effectively support the control

system and improve performance (e.g., reduction of emissions and gas consumption).

The adoption of a neural system of the “mathematical functions simulator” type has proposed a prototype for the "black box" modeling of the cogeneration system. The choice was to model with training the relationship that, using the appropriate commands, links the input parameters to the objectives to be maximized / minimized.

As shown in the Validation section, the neural control prototype proposed for the “analysis and management of thermal sources in the application domain” can effectively simulate the behavior of the boiler system - heating system and model with training the structural differences of the various subsystems.

The training and validation phases carried out on the model, which have given positive results, will, however, be conditioned on the availability of real data, recorded by the system, which were not available. In fact, to formulate and train the prototype, synthetic data taken from the relevant literature have been used. Therefore, the considerations made will to be re-validated in the real context.

It has been seen from the literature that the introduction of thermostatic valves, energy savings can reach up to 40% (TATANO s.n.c., 2020), and the use of the control unit of the system is able to further increase the efficiency of the cogeneration plant. In fact, from the papers (Pretolani, 2003) (Pretolani & Tassi, 2000a) (Pretolani & Tassi, 2000b) (Sarunac, et al., 2003), it can be inferred that the benefits of applying the control system could lead to a further reduction of 0.3 ÷ 2.0% in the specific fuel consumption; moreover, a reduction of 10 ÷ 20% in polluting emissions is expected as well, with a return on investment within the first year of use.

Compared to the sample used for training, the analysis reported in the previous sections has shown that the system can achieve an effective minimization of emissions, correlated with a maximization of the boiler efficiency. However, it is well known that the performance of the Neural Network strongly depends on the Set of examples chosen for training and that the behavior of the proposed system could change with real data.

The training Dataset was generated from few literature data and is limited to the prototype used for this study. It must be adapted to the real data that the network has to learn and in which it will be validated and used.

The adoption of a neural control subsystem has the advantage of making the architecture of the control unit independent from the control subsystem which can be considered as a “black box”, whose possible changes have no impact on the rest of the subsystems, which are part of the ecosystem. Once a complete real Dataset will be available, it might be possible to improve the behavior of the control unit without redesigning the other components.

Conclusions

The objective of this research activity is the application of Artificial Neural Network technologies in the context of two different energy systems for generating mechanical, electrical and thermal energy, namely:

i. Diesel Engine in the Automotive sector;
ii. Boiler of microcogeneration system for residential buildings.

The research activity, conducted in the context of Diesel Engine in Automotive sector, has given as result that the Neural Networks analyzed show a good representation in terms of continuity and generalizability, for the modeling of consumption, performance and emissions. The operating points provided for the training phase are representative of the entire operative plan and can be used for a network prototype to be implemented in the control unit.

Therefore, two possible future scenarios can be outlined:

1. Implementation of on-board vehicle networks, able to improve its accuracy by acquiring new training data from vehicle sensors;
2. Use of these models as objective functions for optimization algorithms with the aim of simplifying the experimental tests.

In the context of MicroCHP Systems, it has been proposed the adoption of a neural system of the “mathematical functions simulator”, a prototype for the "black box" modeling of the cogeneration system was also proposed.

The choice was to model the relationship that links the input parameters to the objectives to be maximized/minimized by properly training the networks. The neural control prototype proposed for the “analysis and management of thermal sources in the application domain” can effectively simulate the behavior of the boiler system. The training and validation phases carried out on the model, which have given positive results, was however conditioned by the availability of real data, recorded by the system, which were not currently available. The study was conducted by exploiting the literature data, instead.

It has been demonstrated that the expected benefits are both in energy savings, that can reach up to 40% by using electronic thermostatic valves and

in the benefits resulting from the application of an electronic control system, so obtaining a 0.3 ÷ 2.0% reduction in specific consumption, and a 10 ÷ 20% reduction in polluting emissions.

Bibliography

ARPA FVG , 2019. *ARPA FVG - Monossido di Carbonio.* [Online] Available at: http://cmsarpa.regione.fvg.it/cms/tema/aria/stato/Qualita_dell_aria/monossido_carbonio.html

Arsie, I., Di Genova, F., Pianese, C., Sorrentino, M., Rizzo, G., Caraceni, A. & Flauti, G., 2004. Development and Identification of Phenomenological Models for Combustion and Emissions of Common Rail Multi-Jet Diesel Engines.. *SAE Paper 2004-01-1877.*.

Arsie, I., Flora, R., Pianese, C., Rizzo, G. & Serra, G., 1999. *A Hierarchical System of Models for The Optimal Design of Control Strategies in Spark Ignition Automotive Engines.* s.l., s.n., pp. Paper No.P-8b-01-4.

Arsie, I., Marotta, F., Pianese, C. & Rizzo, G., 2001. Information Based Selection of Neural Networks Training Data for S.I. Engine Mapping. *SAE Paper 2001-01-0561.*

Arsie, Ivan, Pianese, Cesare, Rizzo, Gianfranco, Flora, Roberto & Serra, Gabriele, 2000. A Computer Code for S.I. Engine Control and Powertrain Simulation. *SAE 2000-01-0938.*

Beale, H. M., Hagan, M. T. & Demuth, H. B., 2017. *Neural Networks ToolboxTM User's Guide.* MathWorks.

Beale, M. H., Hagan, M. T. & Demuth, H. B., 2017. *Neural Networks ToolboxTM Getting Started.* MathWorks.

Belgiorno, G., Di Blasio, G. & Beatrice, C., 2018. Parametric study and optimization of the main engine calibration parameters and compression ratio of a methane-diesel dual fuel engine. *ELSEVIER Fuel 222,* pp. 821-840.

Bianchi, M., Bianchini, L., De Pascale, A. & Peretto, A., 2014. Application of environmental performance assessment of CHP systems with local and global approaches. *Applied Energy,* Volume 130, pp. 774-782.

Cernuschi, S. & Consonni, S., 2016. *E.C.A.T.E., Efficienza e Compatibilità Ambientale delle Tecnologie Energetiche.*

CESI, 2014. *Analisi di fattibilità della applicazione di tecniche di intelligenza artificiale alla ottimizzazione di combustione su un impianto termoelettrico a carbone.* [Online]

Available at:
http://www.ricercadisistema.it:8080/site/binaries/content/assets/rse-sola-lettura/pregresso/2006/Tecnologie_innovative_che_migliorino_le_prestazioni_ambientali_delle_centrali_a_polverinodi_carbone/8b964d 1c-0585-40e6-b371-956dea193ee3_copertina.pdf

CESI, 2015. *Analisi di fattibilità della applicazione di tecniche di intelligenza artificiale alla ottimizzazione di combustione su un impianto termoelettrico a carbone.* [Online]
Available at:
http://www.ricercadisistema.it:8080/site/binaries/content/assets/rse-sola-lettura/pregresso/2006/Tecnologie_innovative_che_migliorino_le_prestazioni_ambientali_delle_centrali_a_polverino _di_carbone/8b964d1c-0585-40e6-b371-956dea193ee3_copertina.pdf

Chen, T.-M., Kuschner, W. G., Gokhale, J. & Shofer, S., 2007. Outdoor Air Pollution: Nitrogen Dioxide, Sulfur Dioxide, and Carbon Monoxide Health Effects. *The American Journal of the medical Science,* Volume 333, pp. 249-256.

CNAE Energia, 2015. *Caldaie a condensazione.* [Online] Available at:
http://www.cnaenergia.it/files/caldaie_condensazione.pdf

CODE 2, 2014. *Micro-CHP potential analysis European level report.*

Cutler, D., Dean, J., Acosta, J. & Jones, D., 2014. *Condensing Boilers Evaluation: Retrofit and New Construction Applications.* National Renewable Energy Laboratory, U.S. General Services Administration.

Di Leo, R., 2015. *PhD Thesis. 'Optimal tuning of control variables in CR Diesel engines via Multi-Zone modelling of combustion and emissions with experimental testing'.* Salerno: University of Salerno.

Energia zero, 2017. [Online]
Available at http://www.energiazero.org/excel/caldaia_condensazione.pdf

European Enviroment Agency, 2010. *Combined Heat and Power CHP.* [Online]
Available at:
https://www.eea.europa.eu/data-and-maps/indicators/combined-heat-and-power-chp-1

Haykin, S., 1999. *Neural Networks, a comprehensive foundation, second edition.* Edit. Prentice Hall.

Heaton, J., 2015. *Artificial Intelligence for Humans volume 3: Deep Learning and neural networks ef. 1.0.* Edit. Tracy Heaton.

Hopfield, J. J. & Tank, D. W., 1985. *"Neural" computation of decisions in optimization problems Biological Cybernetics.*

Hornik, K., 1991. *Approximation capabilities of multilayer feedforward networks. Neural Networks.*

Interesting Engineering, 2011. *Interesting Engineering.* [Online] Available at:

https://interestingengineering.com/transportation/the-everlasting-nearly-emission-free-stirling-engine

Kalman, B. & Kwasny, S., 1992. *Why TANH: choosing a sigmoidal function. In Neural networks.*

LEAP, Politecnico di Milanao, s.d. *Caratteristiche Emissive di Utenze Autonome.* [Online]
Available at:
http://www.leap.polimi.it/leap/images/Documenti/Documenti_Ecate/R1_3_3.pdf

LEAP, 2015. *Caratteristiche Emissive di Utenze Autonome ,LEAP Laboratorio Energia e Ambiente Piacenza, politecnico di Milano,.* [Online]
Available at:
http://www.leap.polimi.it/leap/images/Documenti/Documenti_Ecate/R1_3_3.pdf

LEAP, 2015. *Politecnico di Milano.* [Online]
Available at:
http://www.leap.polimi.it/leap/images/Documenti/Documenti_Ecate/R1_3_3.pdf .

Marquardt, D., 1963. An algorithm for least-squares estimation of nonlinear parameters.. *SIAM Journal on Applied Mathematics, 11,* pp. 431-441.

Martinez, S., Michaux, G., Salagnac, P. & Bouvier, J.-L., 2017. Micro-combined heat and power systems (micro-CHP) based on renewable energy sources. *Energy Conversion and Management,* Volume 154, pp. 262-285.

Mastroberti, M. & Pianese, C., 2000. *Identificazione e validazione di modelli a rete neurale per motori ad accensione comandata mediante tecniche monte carlo.* Bari, Matera, 55° Congresso Nazionale ATI, September, 15-20.

McCulloch, W. & Pitts, W., 1943, December 21. *A logical calculus of the ideas immanent in nervous activity. Bulletin of Mathematical Biology,.* s.l.:s.n.

Montgomery, D. C., 2013. *Design and Analysis of experiments, Eight edition.* s.l.:Jhon Wiley & sons Inc..

Morrin, S., 2015. *"Gas Boiler Test Results - Morrin UCD".* [Online]
Available at:
http://erc.epa.ie/safer/resource?id=6e152841-2997-11e1-ad3d-005056ae0019

Mozer, M. C., 1995. *Backpropagation. In Y. Chauvin & D. E. Rumelhart (Eds.),.* Hillsdale, NJ, USA: Erlbaum Associates Inc..

Naso, V., 1991. *La Macchina di Stirling.* s.l.:Editoriale ESA.

Ogur, E. O. & Kariuki, S., 2014. Effect of Car Emissions on Human Health and the Environment. *International Journal of Applied Engineering Research,* 9(21), pp. 11121-11128.

Ordine degli Ingegneri di Cagliari, 2015. *Ordine degli Ingegneri di Cagliari: Impianti ad Alta efficienza.* [Online]
Available at:

http://www.ingegneri-ca.net/materiali/impianti-alta-efficienza

Patterson, D. W., 1999. *Artificial Neural Network, Theory and Applications.* s.l.:Prentice Hall.

Pretolani, F., 2003. *Tecniche di controllo avanzato delle emissioni: sperimentazione su prototipo di un SW di ottimizzazione della efficienza energetica e delle emissioni,* s.l.: CESI A3/005283, February, 20.

Pretolani, F. & Tassi, E., 2000a. *Tecniche di controllo avanzato delle emissioni: analisi dei sistemi disponibili sul mercato e definizione progettuale del sistema innovativo,* CESI A0/023719, 31.05.2000.

Pretolani, F. & Tassi, E., 2000b. *Tecniche di controllo avanzato delle emissioni: valutazione costi benefici e confronto con i sistemi disponibili sul mercato,* CESI A0/023723, 31.06.2000.

Redlich, R. W. & Berchowitz, D. M., 1985, March. "Linear Dynamics of free- piston Stirling Engines". *Proceedings of the Institution of Mechanical Engineers,* March.pp. Vol. 199, No A3.

Riedmiller, M. & Braun, H., 1993. *A direct adaptive method for faster backpropagation learning: The RPROP algorithm..* s.l., s.n.

Rossomando, B., 2020. *Ph.D. Thesis in Industrial Engineering Curriculum in Mechanical Engineering - XXXII Cycle Experimental analysis of PM and PN emissions during accumulation and regeneration of standard and catalytic DPFs in Diesel engines.*

Sarunac, N., Romero, E. C. & Levy, E. K., 2003. *Combustion optimization: Part I – Methodology and tools.* Vancouver (Canada), s.n., pp. September, 21-24.

Sokołowski, M. M., 2020. *European Law on CombinedHeat and Power.* s.l.:Routledge Taylor & Francis Group.

Spriet, J. A. & Vansteenkiste, G. C., 1988. *Modelli matematici e simulazione..* Milano: Gruppo Editoriale Jackson.

TATANO s.n.c., 2020. *Valvole Teromostatiche: cosa sono e quanto si risparmia, Tatano.* [Online]
Available at: https://www.tatano.com/it/blog/risparmio-energetico/valvole-termostatiche-come-funzionano-e-quanto-si-risparmia

The Plan.it, 2012. *VITOWIN 300-W.* [Online]
Available at:
https://www.theplan.it/media/com_form2content/documents/c/a113/f4/VITOTWIN%20300-W%20DEFINITIVO%2006.03.2012.pdf

Thombare, D. G. & Verma, S. K., 2008. Technological development in the Stirling cycle engines. *Renewable and Sustainable Energy Reviews,* 12(1), pp. 1-38.

TiKz.net, 2023. *TiKz.net - Beta Type Stirling Engine.* [Online]
Available at:
https://tikz.net/engine_stirling_beta/

Töbelmann, D. & Wendler, T., 2020. The impact of environmental innovation on carbon dioxide emissions. *Journal of Cleaner Production,* 20 Jenuary.

Tortora, A., 2017. *Ottimizzazione Vincolata delle strategie di controllo per un MCI Diesel CR.* Tesi di Laurea magistrale a cura di s.l.:University of Salerno.

USEPA, 2015. *U.S. Environmental Protection Agency.* [Online] Available at:
http://ampd.epa.gov/ampd/

Wang, J. et al., 2019. Flexibility of combined heat and power plants: A review of technologies and operation strategies. *Applied Energy,* 252(113445).

Werbos, P. J., 1988. *Generalization of backpropagation with application to a recurrent gas market model. Neural Networks.* s.l., s.n.

Wikipedia, 2021. *Cogeneration Wikipedia - The Free Encycolpedia.* [Online]
Available at:
https://en.wikipedia.org/wiki/Cogeneration#References

Zhu, Shunmin, Yu, Guoyao, Liang, Kun, Dai, Wei & Luo, Ercang, 2021. A review of Stirling-engine-based combined heat and power technology. *Applied Energy, Elsevier,* Volume 294 (C).

Symbol list

β_i	*Generic regression coefficient*
ϵ	*Constant regression known term*
η	*Boiler Efficiency*
η_m	*Mechanical Efficiency*
σ	*Standard deviation*
a	*Generic Neuron output*
AFR	*Air Fuel Ratio*
ANN	*Artificial Neural Network*
b	*Generic bias*
BAU	*Business-as-usual*
CAN	*Controller Area Network*
CH_4	*Methane*
CHP	*Combined Heat and Power*
CLD	*Chemi-Luminescence Detector*
CN	*Combustion Noise*
CO	*Carbon Monoxide*
CO_2	*Carbon dioxide*
degBTDC	*degree Before Top Dead Center*
DOC	*Diesel Oxidation Catalyst*
DPF	*Diesel Particulate Filter*

$DT_{(name\ of\ injection)}$	*Dwell time of referred injection (PILOT, PRE, MAIN, AFTER, POST)*
ECU	*Engine Control Unit*
EGR	*Exhaust Gas Recirculation*
EMCON	*Emission Control*
f	*Generic activation function*
f_i	*Value calculated by the Neural Network*
FID	*Flame Ionization Detector*
FSN	*Filter Smoke Number*
GNA	*Gauss-Newton Algorithm*
GHG	*Green House Gas*
H_2	*Dihydrogen*
HC	*Hydrocarbons*
HRR	*Heat Release Rate*
IMEP	*Indicated Mean Effective Pressure*
input	*Number of Neural Network inputs*
k	*Selected number of Hidden Layers*
LMA	*Levenberg-Marquardt Algorithm*
$m_{inj\ TOT}$	*Mass of fuel injected during a thermodynamic cycle*
M_{AIR}	*Mass of air measured during a thermodynamic cycle*
MFBX	*Mass Fraction Burned Angles*
N_{par}	*Number of Neural Network parameters*
N_{neuron_max}	*Maximum number of neuron possible in function of size of experimental Dataset*
N_{point}	*Size of experimental Dataset*
NDIR	*Non Dispersive Infra Red*
n_1	*Number of the neurons in the first Hidden Layer*
n_i	Number of neurons in the *i*th Hidden Layer
n_{i-1}	Number of neurons in the *(i-1)*th Hidden Layer

n_{in}	*Size of input pattern*
n_{out}	*Size of output pattern*
NMCOV	*Non-methane Volatile Organic Compounds*
NEDC	*New European Driving Cycle*
NMHC	*Non-methane hydrocarbon*
NO	*Nitric Oxide*
NO_X	*Nitrogen Oxides*
O	*Athom of Oxigen*
O_2	*Oxigen*
O_3	*Ozone*
output	*Number of Neural Network outputs*
P_{BOOST_ABS}	*Absolute pressure measured at inlet valve*
P_{MAN}	*Pressure in manifold*
P_{rail}	*Rail Pressure*
PM	*Particulate Matter*
p	*Generic neuron input*
p(v)	*Instantaneous pressure inside the cylinder*
$Q_{(name\ of\ injection)}$	*Quantity of fuel injected in a referred injection (PILOT, PRE, MAIN, AFTER, POST)*
Q_{ref}, Q_{tot}	*Total Quantity of fuel injected in a Thermodynamic Cycle*
R^2	*Correlation coefficient*
ReLU	*Rectified Linear Unit*
SCR	*Selective Catalyst Reduction*
$SOI_{(name\ of\ injection)}$	*Start of referred injection (PILOT, PRE, MAIN, AFTER, POST)*
SFC	*Specific Fuel Consumption*
TDC	*Top Dead Center*
V_D	*Displacement*
v	*Instantaneous volume inside the cylinder*

VGT	*Variable Geometry Turbine*
VOC	*Volatile Organic Compounds*
w	*Generic weight*
WTLP	*Worldwide Harmonized Light Vehicles Test Procedures*
x	*generic independent variable*
X	*Generic mass fraction burnt*
y	*Generic dependent variable*
$\bar{y}$	*Arithmetical mean value of measured points*
y_i	*Measured value*
ZrO_2	*Zirconium Oxide*